Investigation of the capability of RANSE CFD for propeller calculation in practical use

Nguyen Manh Chien

Master Thesis

presented in partial fulfillment
of the requirements for the double degree:
"Advanced Master in Naval Architecture" conferred by University of Liege
"Master of Sciences in Applied Mechanics, specialization in Hydrodynamics,
Energetics and Propulsion" conferred by Ecole Centrale de Nantes

developed at University of Rostock
in the framework of the

"EMSHIP"
Erasmus Mundus Master Course
in "Integrated Advanced Ship Design"

Ref. 159652-1-2009-1-BE-ERA MUNDUS-EMMC

Supervisor: Prof. Nikolai Kornev, University of Rostock

Reviewer: Dr. Pierre-Emmanuel Guillerm, Ecole Centrale de Nantes

Rostock, February 2015

ABSTRACT

Nowadays, Reynolds-averaged Navier–Stokes equations (RANSE) is a viable approach to effectively analyze the performance of ships on a large range of different operating conditions. In DNVGL - Futureship Potsdam, by using commercial full RANSE code ISIS - CFD (integrated in Numeca Fine/Marine software), a high degree of accuracy and relatively short computation times can be achieved for pure resistance calculations. However, propulsion computations - taking into account interaction of a working propeller and the hull - are still subjected to large restrictions. Currently, they are using the simple propeller model (the method called: body force approach) to predict the performance of a hull in self-propulsion condition. It provides capable to assess the effects of the propeller on the hull, while maintaining a low computational effort. However, the propeller thrust, torque and relative rotative efficiency are not accessible. It influences on the total power consumption of a vessel in a certain operation conditions.

For that reason, the main work of this thesis is to investigate the capability of different propeller modeling approaches in RANSE CFD for practical application or daily using. Therefore, the balance between the computational time and level of accuracy need to be taken into account. The ISIS - CFD code - the "daily use" code in DNVGL Potsdam - is used. Two steps need to be included in the investigation as follows:

- Setup of a simulation with rotating propeller for an open water test and then evaluation of the results. Some methods are available to do open water test; therefore this step also include the selection of most efficient method. Besides, different turbulence model are also tested.

- Setup of an integrated run with fully rotating propeller behind a ship for a self-propulsion test and evaluation of the results (comparing with experiment data, assessment of the feasibility and practical application). At first, the simulation is carried out for a ship without rudder; then a dummy rudder is added to the hull form to perform simulation and evaluate the influence of rudder to the result.

Nguyen Manh Chien

Master's Thesis developed at the University of Rostock

CONTENTS

LIST OF FIGURES

LIST OF TABLES

Nguyen Manh Chien

Master's Thesis developed at the University of Rostock

Declaration of Authorship

I declare that this thesis and the work presented in it are my own and have been generated by me as the result of my own original research.

Where I have consulted the published work of others, this is always clearly attributed.

Where I have quoted from the work of others, the source is always given. With the exception of such quotations, this thesis is entirely my own work.

I have acknowledged all main sources of help.

Where the thesis is based on work done by myself jointly with others, I have made clear exactly what was done by others and what I have contributed myself.

This thesis contains no material that has been submitted previously, in whole or in part, for the award of any other academic degree or diploma.

I cede copyright of the thesis in favour of the University of Rostock

Date: January 15, 2015   *Signature*

Nguyen Manh Chien

Master's Thesis developed at the University of Rostock

1. INTRODUCTION

Among some methods available to predict required power for a ship, model tests widely accepted as most reliable means, and could be considered as the closest method to reality. However, due to time and cost for making testing models, it is not suitable for optimization process; it is just only used to validate the result of optimization. Besides, with the rapid improvement of computational resources, Computational Fluid Dynamic (CFD) is getting to become a useful tool in ship design and power prediction. CFD method is able to look into local flow properties and providing a room for designers to improve the design. In DNVGL, they have succeeded to estimate pure resistance of the ship with high level of accuracy and short computational time by using CFD tools. The further step is investigation of the capability of CFD method for prediction the performance of a ship with a rotating propeller behind. It is important because the propulsion parameters (such as: propeller thrust, torque and relative rotative efficiency) influence on the total power consumption.

Figure 1.1 illustrates some approaches for CFD method. In this thesis, we are going to do the simulation with RANSE solver, which is more and more become widely use, due to the balance between computational resources and accuracy. The ISIS – solver developed in commercial software: Numeca Fine Marine is used.
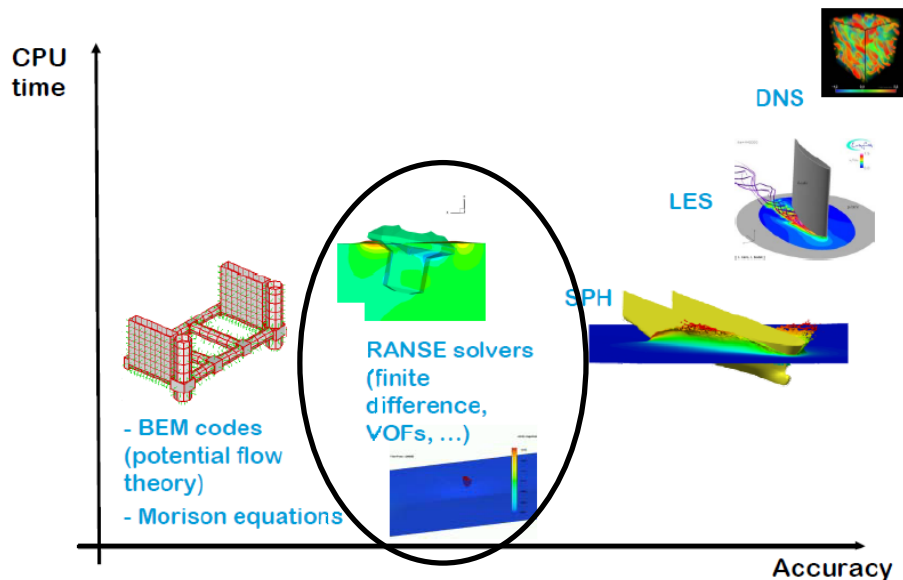
Figure 1.1: Some approachs for CFD [1]

The propeller works behind the ship, however, calculation the performance of the propeller in open water (only the propeller rotates in uniform flow) is also necessary. The open water characteristic of propeller is used in calculation cf propeller working with ship. Therefore, there are two main parts in this thesis: open water calculation and propeller behind ship calculation.

In the first part, 3 methods to do open water simulation are investigated: Sliding Grid, Rotating Reference Frame, and the last one is whole calculation domain rotating with propeller (called Rotating Domain in this thesis). Validating the result is by comparing with experiment test. Moreover, different turbulence models, simulation with Laminar Flow and high Reynolds number are also performed.

The second part deals with rotating propeller behind the ship with Sliding Grid method. The investigation of Sliding Grid for open water test in first part is the base step to do the second part. There are two main types of simulation: propeller rotating behind hull without and with rudder. Only the dummy rudder is added to simulation to see the influence of rudder. The experiment result is available to validate the simulation. At the end, assessments and evaluations are given about the computational resources, level of accuracy and the practical use of simulation. Post processing is also done to see the flow characteristics around the propeller, such as: vortex, streamline…

2. LITERATURE REVIEW

The theory using through the thesis will be briefly summarized in this chapter, with short introduction of ISIS flow solver, and methods using for open water (Sliding Grid and Rotating Reference Frame). Moreover, the open water characteristic of propeller, the interaction of propeller behind the ship and self - propulsion test will be also introduced

2.1. ISIS Flow Solver

2.1.1. Introduction

The ISIS flow solver is a solver based on incompressible unsteady Reynolds – averaged Navier-Stokes equation (RANSE) and developed by *Laboratoire de Mécanique des Fluides, Ecole Centrale de Nantes, France*. Finite volume method is used in the solver for discretization of fluid domain. The velocity field and pressure field are obtained by solving momentum and mass conservation equation

Mass conservation (continuity equation): mass is neither created nor destroyed

$$\frac{d}{dt} \iiint_D \rho dv = 0 \quad \textit{(2.1)} \ [2]$$

Momentum conservation (Newton second's law): rate of change of momentum equal to force

$$\frac{d}{dt} \iiint_D \rho \vec{U} dv = \iiint_D \rho \vec{f_v} dv + \iint_D \vec{T} dS \quad \textit{(2.2)} \ [2]$$

where: dv = arbitrary control volume

ρ = fluid density

D: fluid domain

$\vec{f}_v$ = volume force (normally gravity force)

$\vec{T}$ = constraints. $\vec{T} = \overline{\overline{\sigma}}.\vec{n}$, where: $\overline{\overline{\sigma}}$ = constraint tensor

2.1.2. Turbulent model using in thesis

In nature, most of flows are turbulent. Turbulence is the features of flow, not the physical characteristic of fluid itself. Nowadays, there are many methods available to describe turbulent flow, such as: Direct Numerical Simulation (DNS), Large Eddy Simulation (LES), Detached Eddy Simulation (DES) or based on the Reynolds-Average Navier-Stokes equations (RANSE). However, for most of industrial problems, engineers are usually interested in the mean field of flow. Therefore, recently, RANSE method is used widely in practical purpose, to solve many range of problem.

Basically, in RANSE method, the instantaneous characteristics of flow are decomposed into mean and fluctuated quantities, particularly for velocity field and pressure field, respectively:

$$\vec{U} = \overline{\vec{U}} + \vec{u}' \text{ and } \vec{p} = \overline{\vec{p}} + \vec{p}' \text{ (2.3)}$$

That leads to RANSE equation:

$$\frac{\partial \overline{U_i}}{\partial x_i} = 0 \text{ (2.4) [2]}$$

$$\frac{\partial \overline{U_i}}{\partial t} + \overline{U_j} \frac{\partial \overline{U_i}}{\partial x_j} = -\frac{1}{\rho} \frac{\partial \overline{p}}{\partial x_i} + \frac{\partial}{\partial x_j} (v \frac{\partial \overline{U_i}}{\partial x_j} - \overline{u'_i u'_j}) \text{ (2.5) [2]}$$

In momentum equation after taking average (equation 2.5), there is one additional stress: $\overline{u'_i u'_j}$: called Reynolds stresses, and it has to be determined. The process of specifying Reynolds stresses is called turbulence model or turbulence closure.

In this thesis, there are two kinds of turbulence model which is used to solve RANSE equation:

- Eddy Viscosity model (two-equation: k-ε; k − ω)
- Reynolds-Stress Transport Models

Some short introductions of turbulence model are going to be described in the following parts.

2.1.2.1. Eddy Viscosity model

Using of eddy viscosity model is very popular nowadays because they are simple to code (compared to other models), and very effective in solving normal engineering flows. The model is based on Boussinesq hypothesis: Reynolds stresses are defined through velocity gradient and eddy viscosity, particularly:

$$-\overline{u'_i u'_j} = -\frac{2}{3} k \delta_{ij} + v_t (\frac{\partial \overline{U_i}}{\partial x_j} + \frac{\partial \overline{U_j}}{\partial x_i}) \text{ (2.6) [2]}$$

With Bousinesq hypothesis, there are only two unknowns need to be solved: k (Turbulent kinetic energy) and v_t (kinematic eddy viscosity; or $\mu_t = \rho v_t$ called by eddy viscosity). There are several methods to determine k and μ_t, that leads to different turbulence models. Among them, turbulence models using two transport equation (v_t is determined from two variables) are widely used. In this thesis, some typical two transport equation turbulence models will be used: k-ε , k-ω SST Menter and k-ω BSL

*) k-ε model: The turbulent eddy viscosity μ_t is determined by: $\mu_t = \rho C_\mu \frac{k}{\varepsilon}$ (2.7)

Two variables here are: k and ε, C_μ: constant number = 0.09

where k is Turbulent kinetic energy and ε is the rate of dissipation .These variables will be determined by solving two transport equations.

*) k-ω model (Based D.C Wilcox) [3]:

Instead of ε, the second variable is ω; and turbulent eddy viscosity $\mu_t = \rho \dfrac{k}{\omega}$ *(2.8)*

As the k-ε model; k and ω will also be solved from two transport equations (but different from k-ε model)

*) k-ω SST (Shear – Stress transport) Menter:

Compared to k-ω model (Based D.C Wilcox [3]), the transport equations are the same, but there is a modification of the expression of turbulent eddy viscosity μ_t

$$\mu_t = \frac{\rho K / \omega}{\max\{1, \Omega F_2 / (a_1 \omega)\}} \quad (2.9) \ [4]$$

With a_1 is constant = 0.31, Ω is vorticity, F_2 is auxiliary function, is defined from the distance to the wall d:

$$F_2 = \tanh\left(\left[\max\left\{2\frac{\sqrt{k}}{0.09 d\omega}, \frac{500\mu}{\rho d^2 \omega}\right\}\right]^2\right) \quad (2.10) \ [4]$$

The terms: $\max\{1, \Omega F_2 / (a_1 \omega)\}$ limits the maximum value of μ_t *"by forcing the turbulent shear stress to be bounded by the turbulent kinetic energy times a_1"* [4]

*) k-ω BSL (Base - line model)

This is the "blending model" between k-ω and k-ε: for the area close to the wall: using k-ε, in the far field the k-ω expression is used. Because k-ε and k-ω are solved by different transport equation, hence there is necessary to introduce a so called: blending function.

The auxiliary blending function F_1 is defined as:

$$F_1 = \tanh\left(\left[\min\left\{\max\left\{\frac{\sqrt{K}}{0.09 d\omega}, \frac{500\mu}{\rho d^2 \omega}\right\}, \frac{4\rho \sigma_{\omega 2} k}{CD_{k\omega} d^2}\right\}\right]^4\right) \quad (2.11) \ [4]$$

$$with \quad CD_{k\omega} = \max\left\{\frac{2\rho \sigma_{\omega 2}}{\omega} \frac{\partial K}{\partial x_j} \frac{\partial \omega}{\partial x_j}, 10^{-20}\right\}$$

$CD_{k\omega}$ is called cross-diffusion in the k-ω model.

2.1.2.2. Reynolds-Stress Transport Models

Although the 2 equations turbulence model (k-ω and k-ε) is widely used in many hydrodynamic problems nowadays, in some cases they still show limitation. They only model

the sum of normal turbulent stresses through k (turbulent kinetic energy), not individual one. In addition, some simulations with two-equation turbulence model show the bad result on flows with intense longitudinal vortices [4]. That leads to the appearance of Reynolds Stress Transport Models (RSTM) to build the exact transport equations for the Reynolds stress:

$$\frac{\partial}{\partial t}\left(\rho \overline{u_i' u_j'}\right) + \frac{\partial}{\partial x_k}\left(\rho U_k \overline{u_i' u_j'}\right) = P_{ij} + \Phi_{ij} - \varepsilon_{ij} + \frac{\partial}{\partial x_k}\left(C_{ijk} + \mu \frac{\partial}{\partial x_k} \overline{u_i' u_j'}\right) \quad (2.12) \text{ [4]}$$

Where: P_{ij} is production terms: exact and not require modelling

Φ_{ij} : pressure-strain tensor

C_{ijk} : third order diffusion correlation, and will be modelled

ε_{ij} : dissipation rate

According to the theoretical manual of ISIS solver, using RTSM model normally will double computational time [4]. However, RTSM model is more exact but needs strong closure hypothesis to be used in practical (pressure-strain, dissipation…). Therefore, common practical approach is Explicit Algebraic Stress Models (EASM), which are *"derived from equilibrium hypotheses imposed on the convective and diffusive terms in the RST equation"* [4]. Because of the complexity in the equation and implementation of this model, and the practical direction of this thesis, detail theory will not be introduced here. Nevertheless, in this thesis, EASM turbulence models will be used to compare the result with other Eddy Viscosity models.

2.1.3. Sliding Grid approach

Sliding Grid is the common approach to describe the rotational motion of fluids. In this method, there often have two parts which are connected together: stationary part and rotating part. The rotating part rotates each every time steps, and the connection between two parts is also re-calculated each time steps. According to the theoretical manual of Fine/ Marine software, to calculate fluxes through the sliding interface, there are no specific interpolation used. Particularly, for the standard cells (non – rotating cells), we have to calculate fluxes in and out the cells. For the cell and face at sliding interface, we search the cell centre (in the other part) that is best match the face. This cell will be used for flux computation as the same as for the standard cells.

The procedure can be described in 3 steps as the figure below [4]
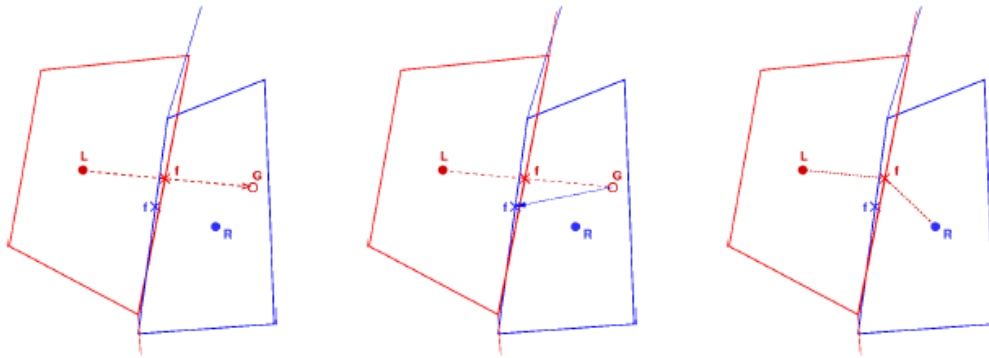
Figure 2.1: Sliding faces: Construction of ghost points (left), searching the global faces (centre), the new neighbour cells (right)[4]

2.1.4. Rotating Reference Frame approach

Another approximately approach to describe the rotating motion is the Rotating Reference Frame. The mesh of rotational part does not have to change its position each time step.
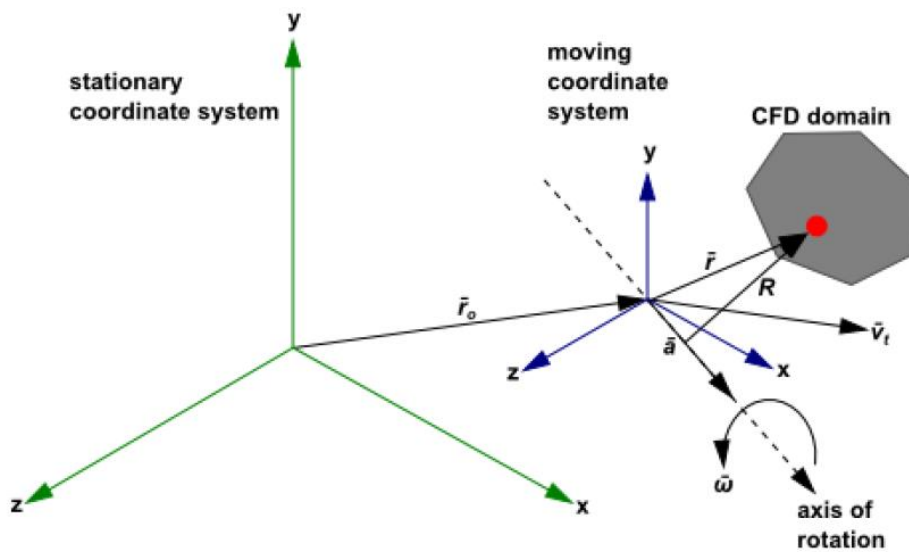
Figure 2.2: Description of rotating reference frame method [5]

The velocity of fluid particles in moving frame can be expressed by:

$$\vec{v_r} = \vec{v} - \vec{u_r} \ (2.13)$$

where:

$$\vec{u_r} = \vec{\omega} \times \vec{r} \ (2.14)$$

$\vec{v_r}$ is the velocity of fluid particles in rotating frame

$\vec{v}$ is absolute velocity (velocity viewed in stationary frame)

$\vec{\omega}$ is angular velocity of rotating frame

The governing equation of motion written in rotating reference frame (using $\vec{v_r}$ instead of $\vec{v}$) as follows:

$$\nabla \cdot \rho \vec{v_r} = 0 \quad (2.15)$$

$$\nabla \cdot (\rho \vec{v_r} \vec{v_r}) + \rho (2\vec{\omega} \times \vec{v_r} + \vec{\omega} \times \vec{\omega} \times \vec{r}) = -\nabla p + \mu \nabla \cdot \nabla (\vec{v_r}) \quad (2.16)$$

In the new momentum equation, there are two additional terms: $(2\vec{\omega} \times \vec{v_r})$: Coriolis term and $(\vec{\omega} \times \vec{\omega} \times \vec{r})$:centripetal acceleration term. The propeller viewed from the rotating reference frame will be stationary. This method can be considered as "a steady approach" for rotating motion, therefore, compared with Sliding Grid, it takes less computational resources.

2.2. Propeller Characteristics

Generally speaking, the performance characteristic of a propeller could be divided into two categories: the open water and self-propulsion properties. Open water characteristics describe the forces and moments acting on the only propeller itself in a uniform flow. Besides, behind hull characteristic is mentioned when we consider the forces and moment which are generated on the propeller working in the mixed wake field behind the ship. This section will shortly introduce both types of these characteristics which are used throughout the thesis.

2.2.1. Open water characteristics

To explore the performance of a propeller in the open water condition, we let the propeller rotate with constant angular velocity, then measure the force and moment acting on the propeller. This kind of experiment is often carried out in towing tank or cavitation tunnel with uniform inflow. Normally, while the angular velocity is kept constant, the inflow coming to propeller is varied for each measurement. Therefore, the results of measurement are different forces (thrust - T) and moments (torque - Q) for different inflow speed (advance velocity v_a).These quantities are expressed into the non-dimensional numbers as follows:

Advance coefficient: $J = \dfrac{v_a}{nD}$ *(2.17)*

Thrust coefficient: $K_T = \dfrac{T}{\rho n^2 D^4}$ *(2.18)*

Torque coefficient: $K_Q = \dfrac{Q}{\rho n^2 D^5}$ *(2.19)*

where: ρ is water density, n is angular velocity (Rad/s) and D is propeller diameter (m)

Besides, the open water efficiency η_o is expressed by:

$$\eta_o = \frac{T v_a}{2\pi n Q_o} = \frac{J}{2\pi} \cdot \frac{K_T}{K_{Qo}} \quad (2.20)$$

Note that these non-dimensional quantities above are established by using principle of dimensional similarity, and they characterize the performance of propeller for a specific geometric configuration. Plotting thrust coefficient , torque coefficient and open water efficiency in one graph against advance coefficient (J) gives us the so called "open water curve or open water diagram" – that is useful for comparing propellers of the same shapes but different sizes. In the other way, open water curve can be applicable to any propeller having the same geometric form [6].

Typical form of open water curve is expressed as follows:
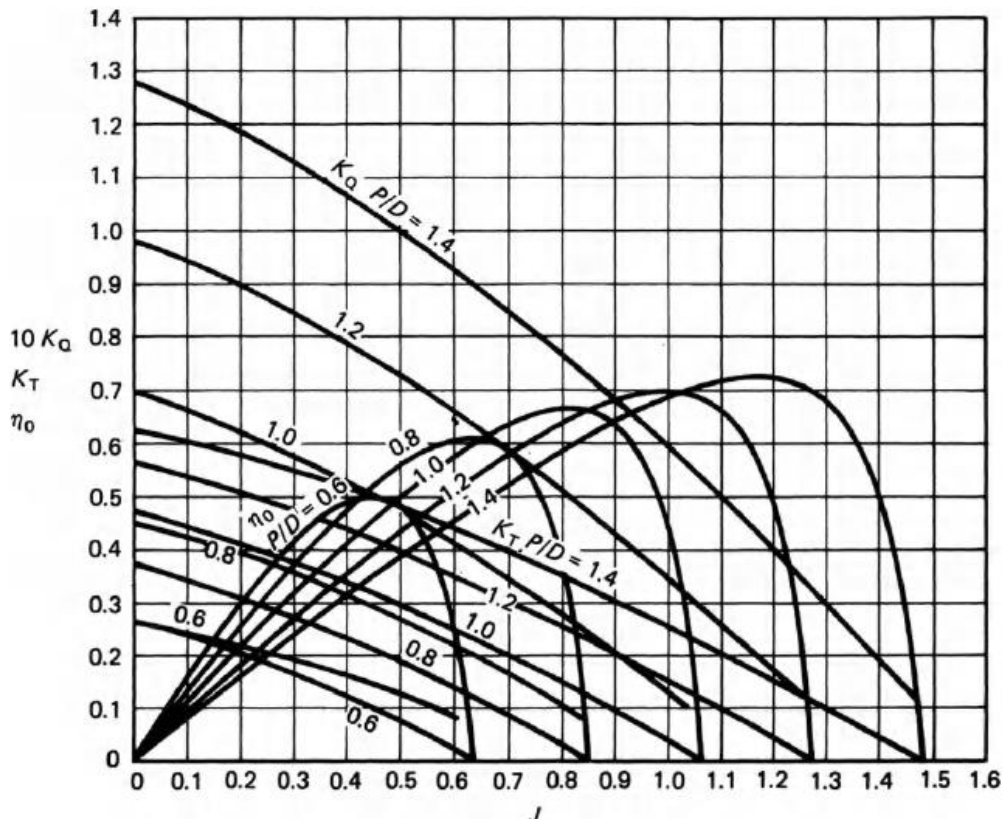
Figure 2.3: Open water diagram for Wageningen B5-75 screw series [6]

2.2.2. Propeller – Hull interaction

As stated above, the behind-hull propeller characteristics are the performance of propeller working in the wake field which is generated behind the ship. In terms of hydrodynamic definition: wake field is caused by the interaction of fluid motion between the hull and flow in the longitudinal direction of hull form. There are several forms to express the wake field data, such as: Velocity Ratio Method, Taylor's method or Froude's method [6]

The common representation of wake field nowadays is the Velocity ratio method. In this method, for a point at propeller plane with axial, tangential and radial velocity, we establish the fraction of these velocities with ship speed to represent the wake field: $\dfrac{v_a}{V_s}; \dfrac{v_t}{V_s} and \dfrac{v_r}{V_s}$
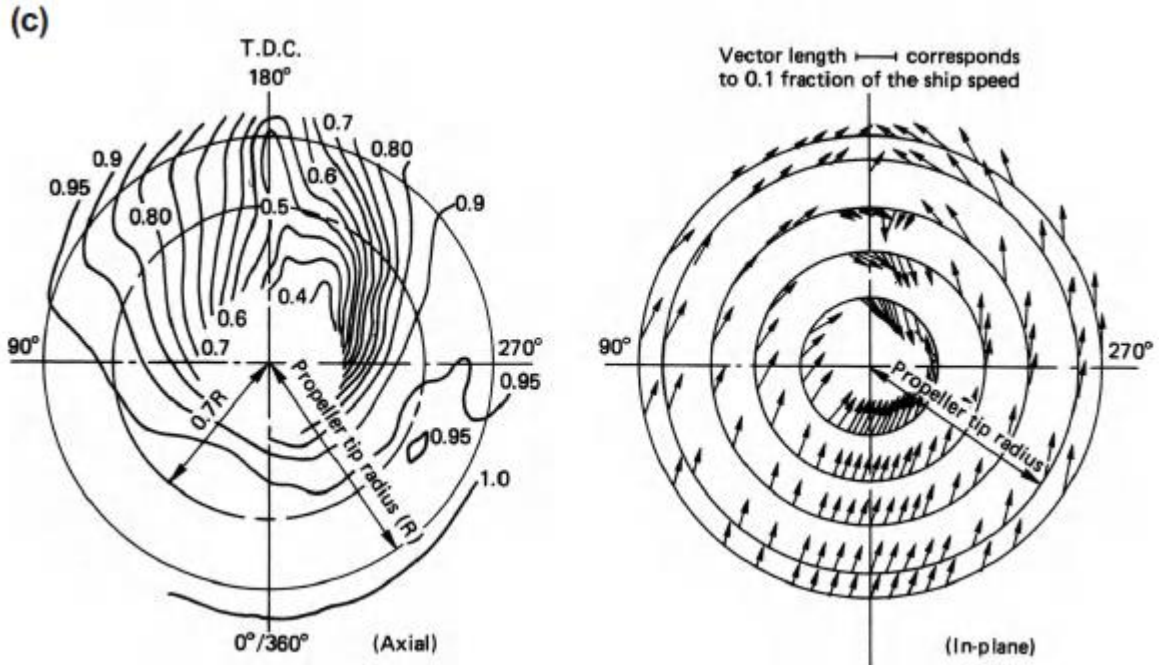
Figure 2.4: Axial and in-plane wake field - twin-screw hull [6]

Besides this method, Taylor introduced the "wake fraction" term

$$w_T = \frac{V_s - v_a}{V_s} = 1 - \frac{v_a}{V_s} \ (2.21)$$

where V_s is ship speed and v_a is speed of advance.

Similar to Taylor, the wake fraction term in Froude method is :

$$w_F = \frac{V_s - v_a}{v_a} = \frac{V_s}{v_a} - 1 (2.22)$$

The wake field measured at propeller plane without the propeller is called nominal wake field; and it can be decomposed as:

$w_n = w_p + w_v + w_w + \Delta w$ *(2.23)*

where :

w_p : the potential wake field – wake field if ship is in non-viscosity fluid

w_v : frictional wake field and arises from – consider the viscous effect of fluid

w_w: wake component due to waves.

Δw: the non-linear part of the wake field

With the presence of the propeller, the wake field behind the hull is modified, hence, there are the interaction between the propeller and hull:

- The propeller increases the flow velocities in the aftbody of the ship

- The propeller decreases the pressure in aftbody

Some important quantities used to characterize the propeller performance behind the ship are as follows:

- Effective power $P_E = R_T \cdot V_s$ *(2.24)* ; it is the power need to use to tow the ship without propeller

- The power generated by propeller is called thrust power: $P_T = T \cdot v_a$ *(2.25)*

- For the self-propelled hull, the pressure at stern decreases, due to the rotation of propeller (giving higher velocity of fluid field). Hence, the thrust T is higher than the resistance R_T , and this difference is expressed through the thrust deduction factor t, which is defined as:

$$t = 1 - \frac{R_T}{T} (\ (2.26)$$

- Taylor's wake fraction: $w_T = \dfrac{V_s - v_a}{V_s} = 1 - \dfrac{v_a}{V_s}$ *(2.27)*

- The hull efficiency: $\eta_H = \dfrac{P_E}{P_T} = \dfrac{R_T \cdot V_s}{T \cdot v_a} = \dfrac{1-t}{1-w}$ *(2.28)*

- The effective power can be expressed by:

$$P_E = \eta_H \eta_o \eta_R \eta_S \cdot P_B \text{ (2.29)}$$

  where η_H : hull efficiency

  η_o : open water efficiency

  η_R: relative rotative propeller efficiency

  η_S: shaft efficiency

In terms of power concerns, the relative rotative propeller efficiency (η_R) is an integral part. It is the fraction between the torque generated by propeller in uniform flow (Q_o) and in the mixed wake field behind the ship (Q).

$$\eta_R = \frac{Q_O}{Q} \text{ (2.30)}$$

The typical value of η_R is from 0.96 to 1.04 [6]

As stated above, the open water efficiency is defined by: $\eta_o = \dfrac{T v_a}{2 \pi n Q_O}$ *(2.31)*

Q_O here means the torque in open water case. If we consider the propeller working behind the ship, the similar term is given and called: behind-hull efficiency: $\eta_B = \dfrac{Tv_a}{2\pi nQ}$ *(2.32)*

Therefore: $\eta_R = \dfrac{\eta_B}{\eta_O}$ *(2.33)*

The reason explaining for the difference between Q_O and Q, or the appearance of relative rotative efficiency η_R could be:

- Difference in fluid field (uniform flow for open water and mixed wake field for propeller behind hull)
- Difference in turbulent flow due to different Reynolds number

2.2.3. Self - Propulsion Test

The self-propulsion test is carried out at towing tank to determine the power demand necessary to (self) propel the ship at a given speed. This test is carried at model scale and is not be extrapolated to full scale. At the end of the test, for calculation of propulsion factors, the open water curve needs to be used. There are two methods available: same torque, or torque identity method and same thrust, or thrust identity method. According to the ITTC procedure [7], normally the thrust identity method is used to get the Torque coefficient from open water curve, then the relative rotative efficiency will be calculated as: $\eta_R = \dfrac{K_{Q_o}}{K_Q}$ *(2.34)*

where: K_{Q_o}: from open water curve using thrust identity method

K_Q: torque coefficient calculated from measurements

In this thesis, the same procedure is carried out, but instead of doing experiment in towing tank, all the necessary data is given by CFD software (Fine/Marine); and the result is compared with experiment data.

3. OPEN WATER SIMULATION

3.1 Propeller Test case

To validate and evaluate the result of open water test, the well – known propeller test case is used. It is Potsdam propeller test case [8]. All the necessary data: the geometry of propeller, experiment test and the CFD result from different solver and institution are available in the website of SVA Potsdam. They are good reference for setup of simulation of compare the result. The Potsdam propeller test case (PPTC) is 5 blades, right handed propeller (look from the pressure side) with some basic dimension as follows:

Diameter	D	0.25 m
Area Ratio	A_E/A_0	0.77896
Skew		18.837 degree
Hub Ratio	d_h/D	0.3
Number of Blades	Z	5
Rotation Direction		R

Table 3.1: Basic dimension of Potsdam Propeller

Modified Geometry: the gap between Hub and Shaft is filled to do the mesh generation
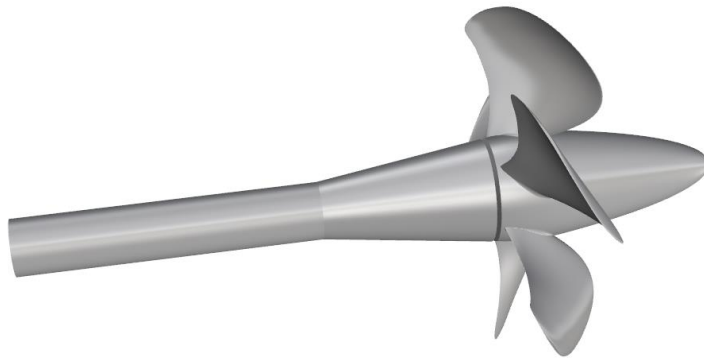
Figure 3.1: Original geometry of Potsdam propeller
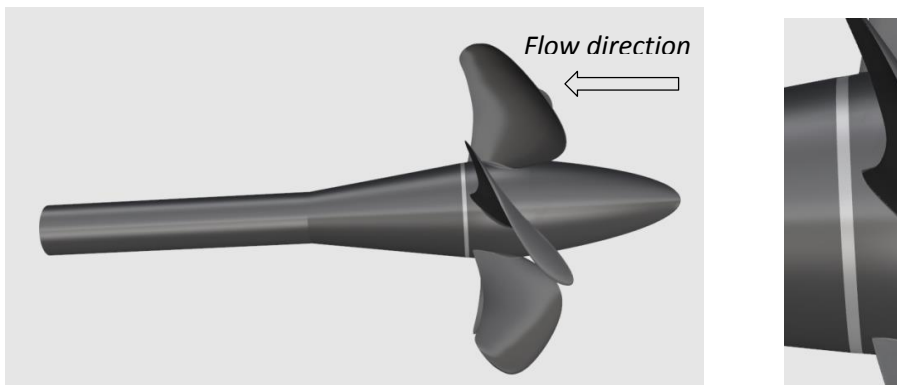
Figure 3.2: Modified geometry of Potsdam propeller

The Cap and the Shaft are arranged oppositely to the normal setup of propeller behind the ship. In this case of open water test, Cap upstream and shaft downstream of propeller plane to avoid the influence of the shaft to the flow coming to the propeller (*see figure 3.2*)

3.2. Mesh generation and Computational Setup

Mesh generation and computational setup are the most time consumption steps. Because many investigations with trial and error process are done in these steps. However, to generate good mesh for simulation, the geometry preparation is also vital. It can be considered as pre-step for mesh generation. In this pre-step, the propeller is divided into some patches: *Shaft, Hub, Cap, Blade coarse mesh and Blade fine mesh, Tip, Fillet*, to be able to provide more flexibility to have different types of mesh with different levels of refinement. Especially, at leading edge and trailing edge of blades, the blade surface has high curvature; the mesh here needs to be refined higher level, to capture the geometry properties. Moreover, to improve the mesh quality, leading edge, trailing edge and tip are also refined (curve refinement). The original geometry does not have curve at leading edge of blade. Thus, extraction leading edge curve step is also done. When the geometry is ready, it is exported to "*Parasolid file format*" to import in Hexpress, for mesh generation.

3.2.1. Mesh generation

As stated above, the open water simulation is carried out by 3 different methods: Rotating Reference Frame, Sliding Grid and the classical approach: whole domain rotating with propeller (in this thesis, we call Rotating Domain). For both two methods (Rotating Domain –RD - and Rotating Reference Frame -RRF), one mesh can be used. The difference between two methods is the simulation setup. Therefore, only two kinds of mesh need to be generated, and for each kind of mesh, there are different numbers of cells to study grid convergence. The major differences between two kinds of mesh is the numbers of domains. There is only 1 domain for Rotating Domain and Rotating Reference Frame method, compared to 2 domains for Sliding Grid.

3.2.1.1. Mesh generation for Rotating Domain method and Rotating Reference Frame

The mesh is hexahedral and mesh is generated by using Hexpress. Detail characteristic of calculation Domain is described in *Figure 3.3*. The Domain is a cylinder with the Diameter equaling 10 times the Propeller Diameter. There is only one domain. First step, the domain is divided by 4704 cells (24x14x14), after that, depending on level of refinement for each area, we can get the different meshes. To study grid convergence, 3 meshes with different number of cells are generated:

Mesh 1: 1.2 million cells

Mesh 2: 3.9 million cells

Mesh 3: 9.0 million cells
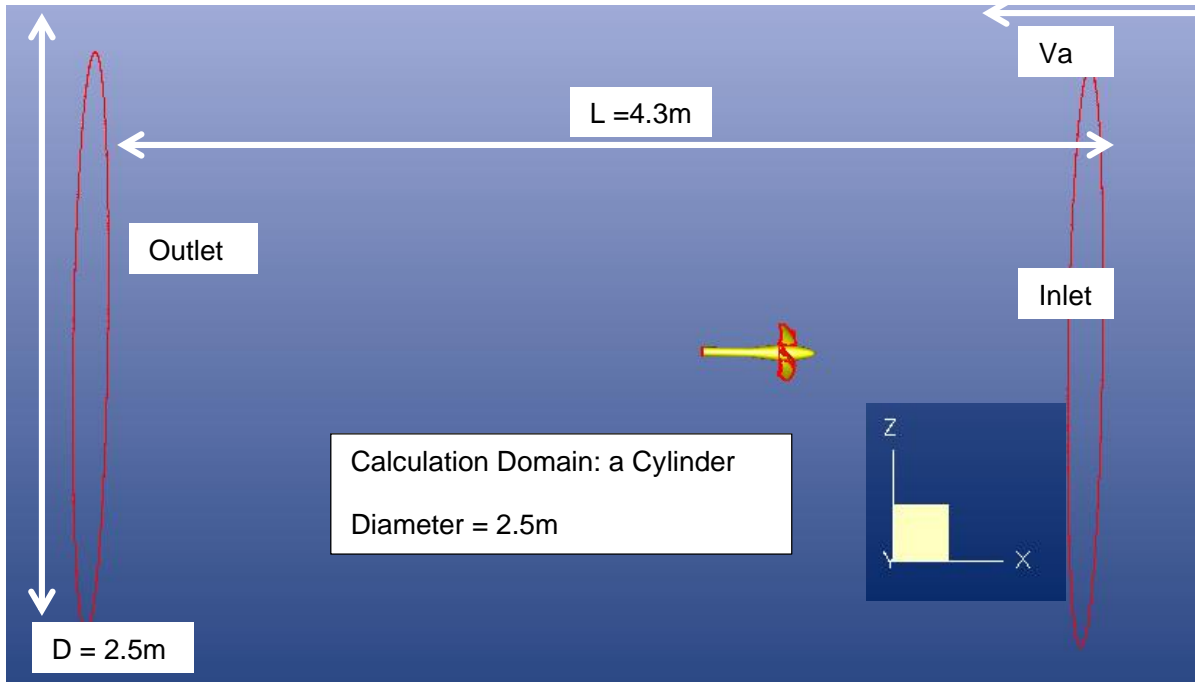
Figure 3.3: Calculation domain for RRF and RD method

The Leading Edge, Trailing Edge and Tips of propeller are much more refined compared to other areas due to complex geometry at these area. The detail of refinement level is illustrated in *Table 3.2* below:

	Refinement Level		
Name of Patch	Mesh 1 (coarse)	Mesh 2 (medium)	Mesh 3 (fine)
Leading Edge (curve)	8	9	10
Trailing Edge (curve)	8	9	10
Tips (surface)	6	8	9
Blade_coarse (surface)	3	4	4
Blade_fine (surface)	5	8	9
Hub (surface)	5	6	7
Cap (surface)	5	6	7
Fillet at root of blade (surface)	5	7	8
Shaft (surface)	3	4	5

Table 3.2: Refinement level for different types of meshes

Hexpress provides some algorithms to improve the mesh quality and they are done automatically. At the end, the mesh should not have any bad quality cells (negative, concave or twisted cells). In case of bad quality cells, after determining the position of these cells, local refinement should be made to improve mesh quality. Even the solver can run with concave or twisted cells, but the computational time will be much higher and besides, accuracy will be lower. For this reason, this step normally consumes time to get a good quality mesh. One more factor leading to time consumption is the number of cells: more cells, more mesh generation time.
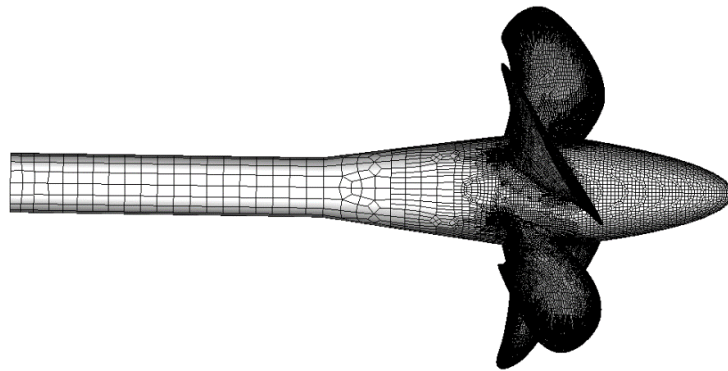
Figure 3.4: Typical mesh of propeller

Figure 3.6 shows the typical mesh for the propeller: more cells at the edge and less cells at the middle areas of blades. The propeller cap is also refined with more cells compare to the shaft to have smooth inflow.

3.2.1.2. Mesh generation for Sliding Grid method

As mentioned above, with sliding grid method, there are two domains: the rotating domain inside the fixed domain *(see Figure 3.5)*. The outer domain has same dimension as RRF method, and the inner one is just small enough to cover whole propeller inside. Between two domains there are common faces (called "Non matching connection face" in Fine Marine). The grid of common face between two domains is not required point-to-point matching each other. This connection enables the solver to compute flux through two domains. For each time step, the inside domain rotates and changes its position, therefore the solver has to re-calculate this connection each time step. The "Non matching connection face" is showed in *Figure 3.6*. This step is done in Hexpress, after mesh generation, if this connection is not established, the Sliding Grid method cannot be completed.
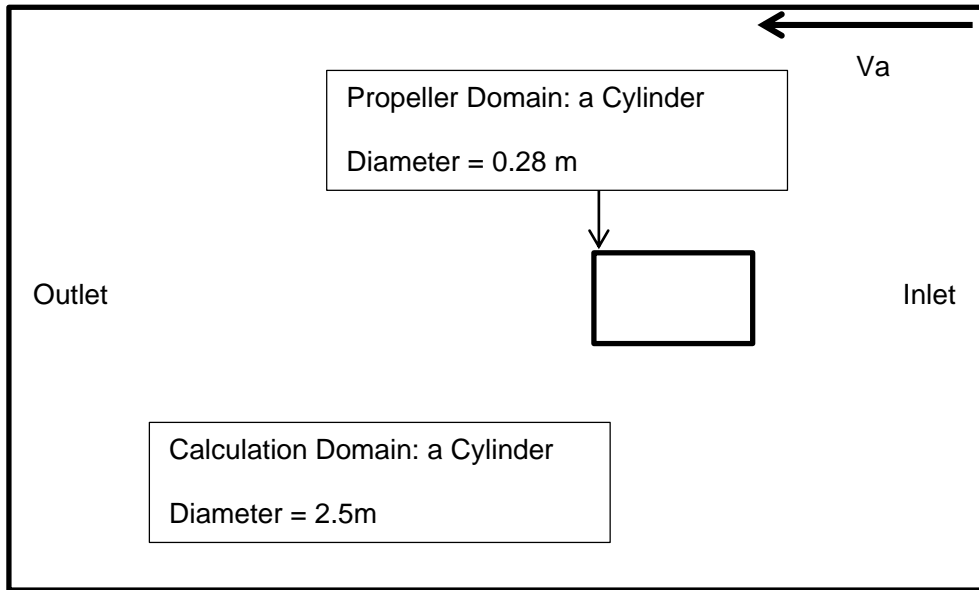
Figure 3.5: Calculation domain for RRF and RD

Similar to the mesh of Rotating Reference Frame method, the initial numbers of cells for domain are kept the same, changing the level of refinement for propeller (local refinement) gives us different mesh sizes. For convergence study, 3 meshes are also created: Mesh 1- 0.8 million cells; Mesh 2 - 3.9 million cells; Mesh 3 - 7.0 million cells. Mesh 2 has same number of cells (3.9 million cells) for all 3 methods. The simulation result with this mesh is used to compare three methods.
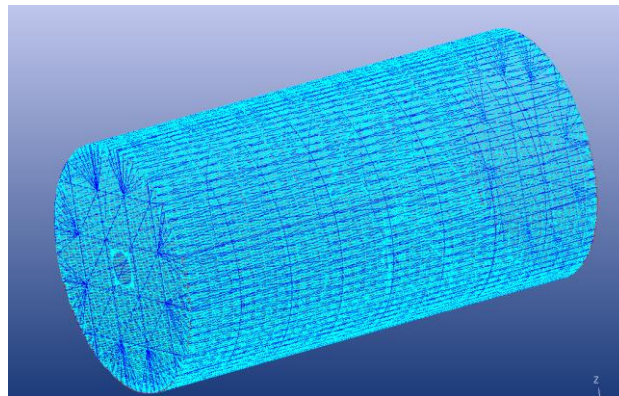
Figure 3.6: Sliding Grid Interface – Full non matching connection

3.2.1.3. Viscous layer insertion

Viscous layer insertion is the last step of mesh generation, and is done by Hexpress. The thickness of viscous layer influents to the computational setup: flow model and boundary condition. Hexpress provides a specific approach to insert viscous layer. The first layer thickness is calculated by the formula: [9]

$$y_{wall} = 6 \left(\frac{V_{ref}}{V} \right)^{-7/8} \left(\frac{L_{ref}}{2} \right)^{1/8} y^+ \quad (3.1) \ [9]$$

where: L_{ref} = reference length = chord length at 0.7R

V_{ref} = reference velocity calculated by:

$$V_{ref} = \sqrt{V_a^2 + (0.7 D \pi n)^2} \quad (3.2)$$

where: D is propeller diameter, n is revolution.

Using above formula, and with the selection of $y^+ = 1$ for propeller blades and $y^+ = 30$ for hub, cap and shaft, viscous layers are calculated. The reason for different selection of y+ is that the flow passes through the blades is much more complicated than other parts. Selecting y+ equals to 1, meaning no wall function is applied, the flow near blades is able to be solved more detailed. This phenomenon can be seen through post processing result with vortex identification, and streamline. Besides, selection of $y^+ = 30$ reduces the number of cells for hub, cap and shaft of propeller, corresponding with wall function is applied in simulation setup.

The viscous layer thickness 3.29×10^{-6} m is set for blades and 3.29×10^{-3} m for hub, cap and shaft. The stretching ratio is selected by 1.2.

3.2.2. Computational Setup

The open water simulation is carried out with different advance coefficient J. We keep constant revolution n = 15 rps for the propeller, J is changed by varying advance velocity Va. Particularly, 5 advance coefficients J is simulated:

Advance velocity Va (m/s)	2.25	3	3.75	4.5	5.25
Advance coefficient J	0.6	0.8	1	1.2	1.4

Table 3.3: List of advance coefficient (J) in Open water simulation

Different turbulent models: k-ω SST, k-ω BSL, k-ε, and EASM are used during simulation, to evaluate the best turbulent model. The same boundary condition is applied for all three methods as follows:

- **Inlet and External boundary:** Far field with advance velocity (Va) imposed
- **Outlet boundary:** Prescribed pressure (frozen pressure)
- **Solid parts:** Wall function approach. When selecting this option, ISIS solver automatically calculates the y^+ to apply appropriate model: wall function or low Reynold number approach. (low y^+).

The major differences in setup of 3 methods are the time step and the number of iteration per time step. This setup directly influences to time consumption or computer resources during simulation. The Rotating reference frame method can be considered as a steady approach for open – water test, therefore large time step and small numbers of iteration is used. Detail setup of time step is as flows:

Method	Number of Iteration per time step	Time step
Rotating Domain	8	0.0003333s (200 time steps per round)
Rotating Reference Frame	4	0.00667s (10 time steps per round)
Sliding Grid	8	0.00013333s (500 time steps per round)

Table 3.4: Time step setup for open water simulation

Computation of the simulation is performed parallel on cluster with 16 cores. For practical use of simulation, computational time or resources is one of the most important aspect. It is a base to assess 3 methods, together with level of accuracy.

3.3. Result

The result is achieved by measuring the force in X direction (thrust) and the moment through X axis (torque) on propeller blades and hub when convergence is reached. The thrust and torque are expressed in non-dimensional forms by K_T and K_Q. After that, the open water efficiency η_O is also calculated.

Basically, convergence criteria in the open water simulation is consider by two factors: the residual of velocity (u,v,w) and pressure are lower than 10^{-4}. And the second factor is: the force and moment also converge. However, generally speaking, when time is going, the force and moment is continuing to fluctuate around one value. Thus, the convergence for force and moment could be considered when they oscillate periodically around a certain value; and the result is achieved by taking average of the force and moment in 1 rotation round of propeller. The two factors mentioned above could be considered as a "basic rule" for achieving convergence in this thesis; but as will present below, the convergence of result also depends on methods, turbulence model and time step used. And this is one of the criterion to evaluate suitable methods using for open water simulation, among computational time and accuracy.

3.3.1. Mesh convergence study

Firstly, grid convergence study is made to see the influence of mesh size to the computational result.

The simulation is carried out with kω-SST turbulence model, using wall function approach. 3 different methods are used: Rotating domain (RD), Rotating Reference Frame (RRF) and Sliding Grid (SG).

Figure 3.7 and Figure 3.8 show the grid convergence study for J = 0.6 and J = 1.4. Generally, speaking, it seems that there is no much influence of mesh size to the result of K_T and K_Q. The difference can be noticeable between coarse mesh and medium mesh. However, the results of simulation for medium mesh and fine mesh are quite similar. For this reason, in the next part of the thesis, the medium mesh (3.9 million cells) is used to compare 3 simulation methods, and also compare with experimental result.

(This area is intentionally left blank)
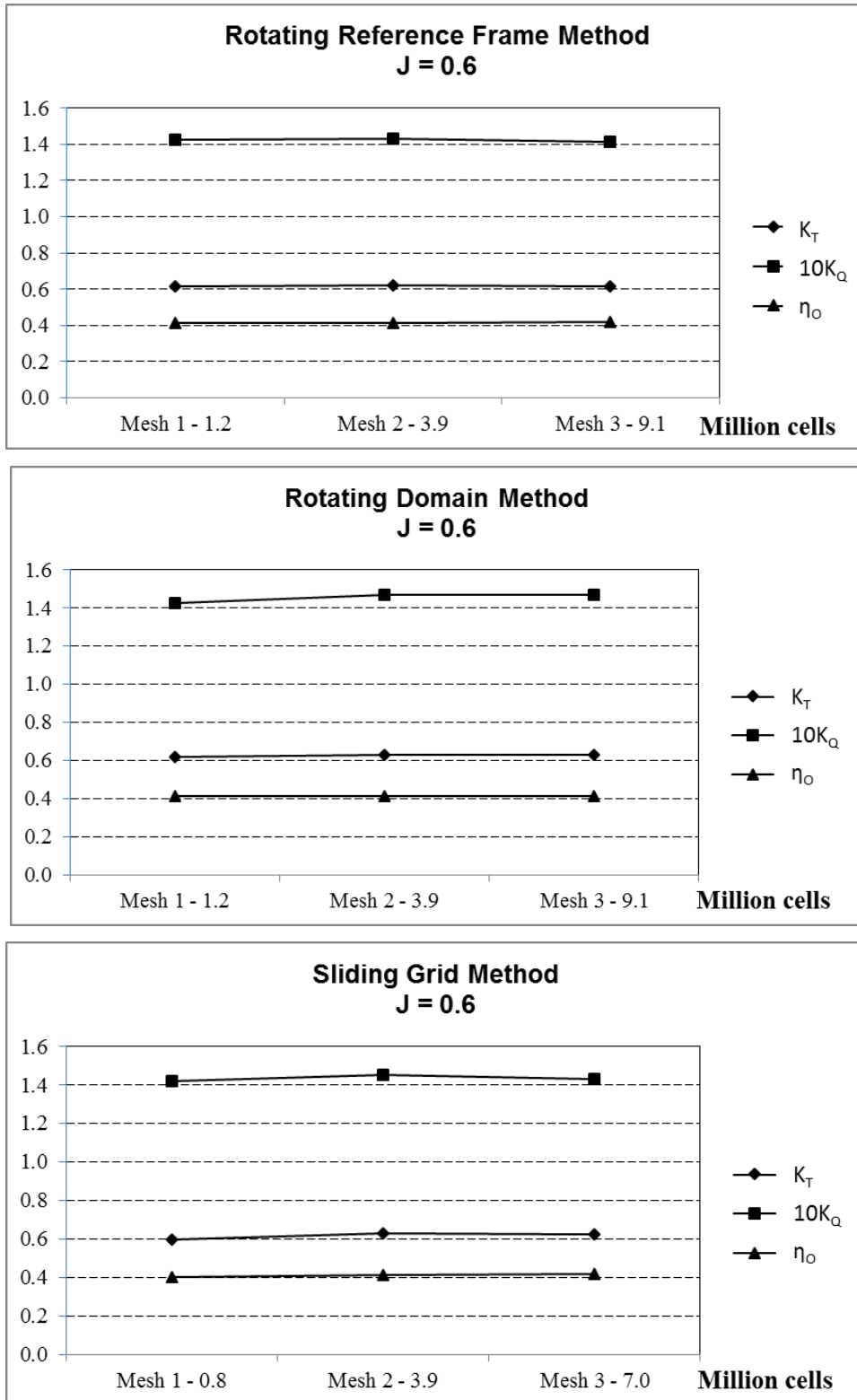
Figure 3.7: Mesh convergence for J = 0.6 with different method
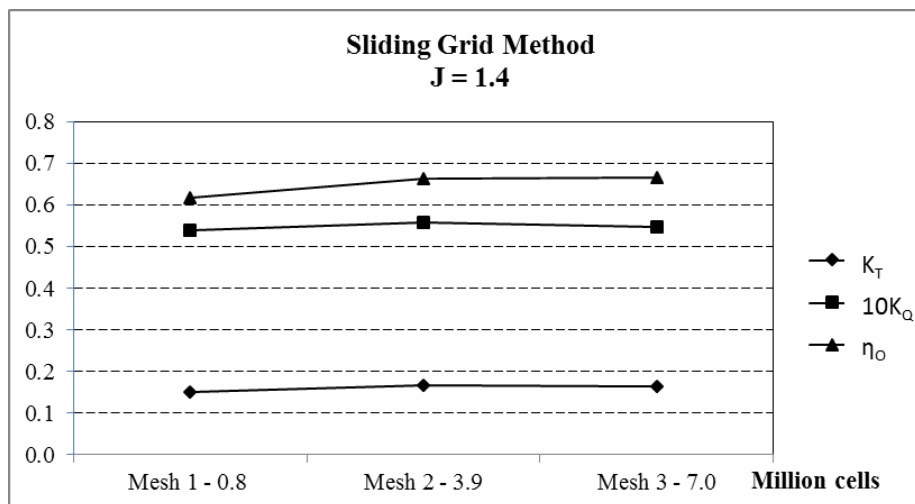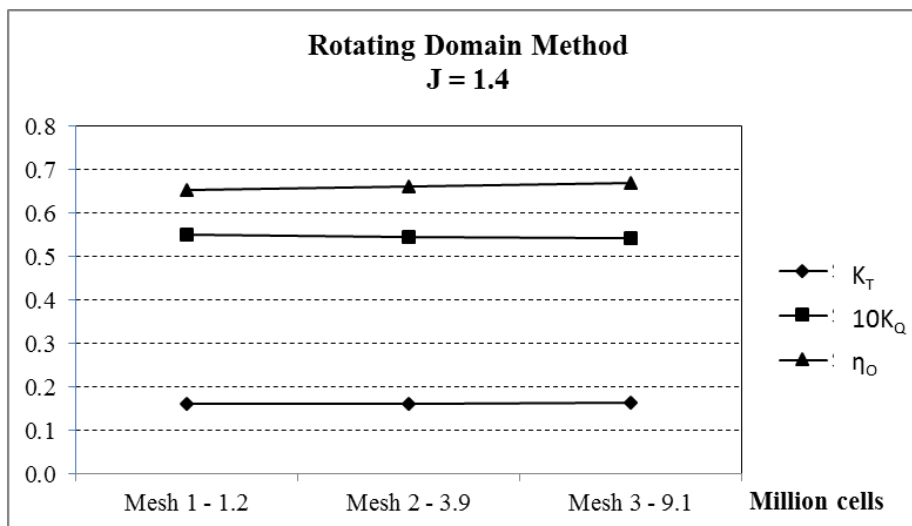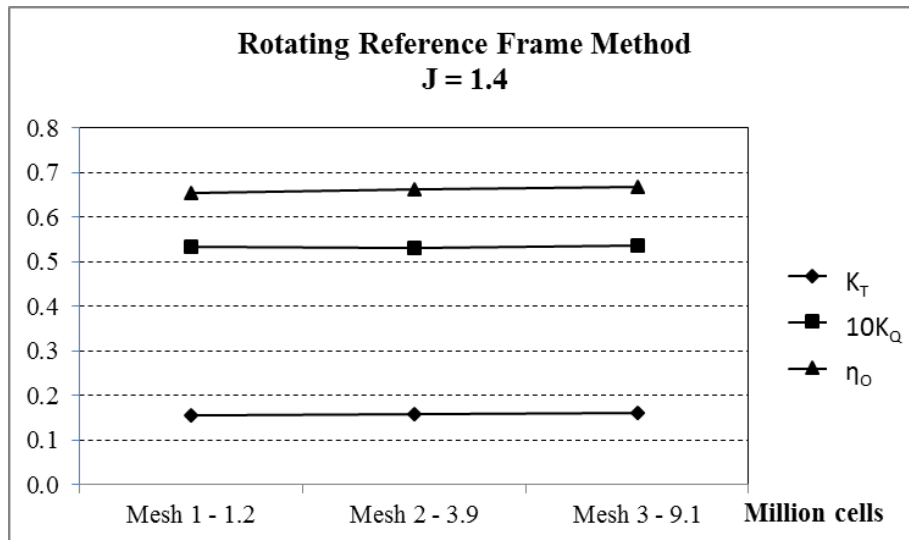
Figure 3.8: Mesh convergence for J = 1.4 with different method

3.3.2. Comparison of 3 methods used for open water simulation

As stated above, 3 methods to simulate open water test are compared by using 3.9 million cells. The factors which are taken into account for comparison are: level of accuracy compared to experimental result, computational time (or computational resources), convergence of result. Moreover, some post - processing are also accomplished to visualize differences in flow properties, such as pressure distribution, tip vortex…

The turbulence model: k-ω SST, wall function approach are used in the simulation. Computation is performed on cluster with 16 cores.

Figure 3.9 below shows the open water curves obtained from 3 methods and also the experimental result. The experimental result (EFD) is expressed in black line. Generally speaking, in terms of numerical result, there is not much difference in 3 methods, and these CFD results are quite close to experimental one. The detail of difference compared to experiment (percentage difference) is shown in *Table 3.5*
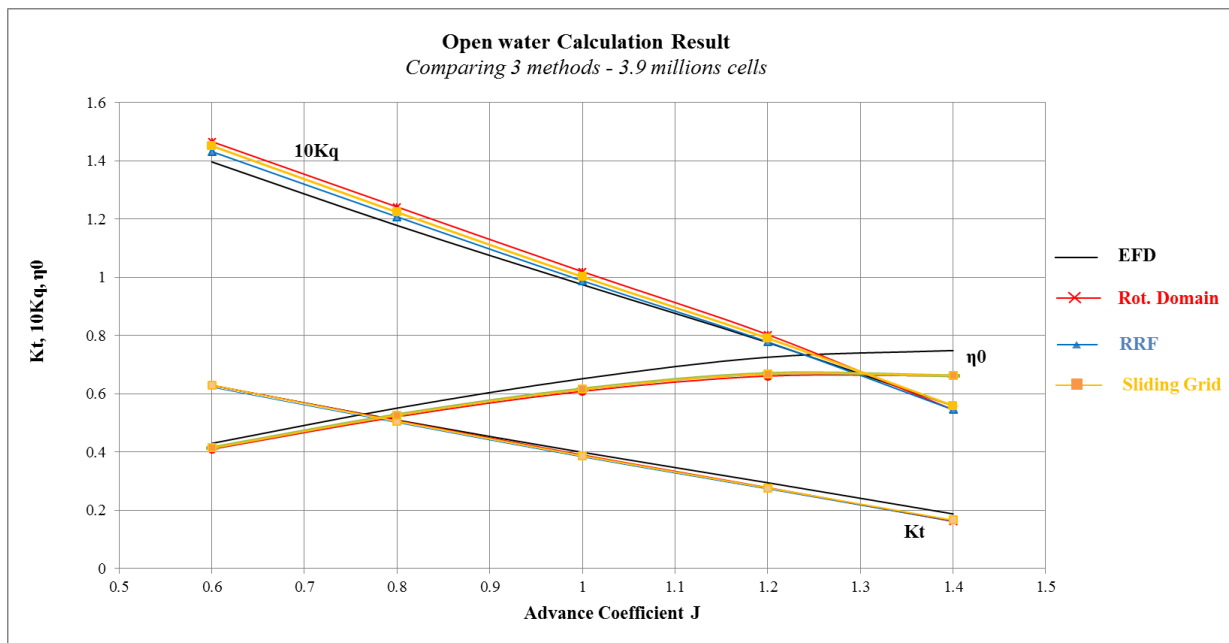
Figure 3.9: Open water curves obtained from different methods

	Sliding Grid		Rotating Domain		Rotating Reference Frame	
J	K_T	ΔK_T	K_T	ΔK_T	K_T	ΔK_T
0.6	0.630	**0.13%**	0.630	**0.12%**	0.623	**-0.99%**
0.8	0.506	**-0.74%**	0.508	**-0.33%**	0.501	**-1.74%**
1.0	0.388	**-2.97%**	0.390	**-2.35%**	0.383	**-4.08%**
1.2	0.277	**-6.06%**	0.278	**-5.72%**	0.273	**-7.39%**
1.4	0.166	**-11.37%**	0.162	**-13.69%**	0.162	**-13.71%**

	Sliding Grid		Rotating Domain		Rotating Reference Frame	
J	K_Q	ΔK_Q	K_Q	ΔK_Q	K_Q	ΔK_Q
0.6	1.451	**3.94%**	1.466	**4.98%**	1.432	**2.53%**
0.8	1.224	**3.88%**	1.242	**5.41%**	1.208	**2.52%**
1.0	1.002	**2.78%**	1.019	**4.57%**	0.988	**1.35%**
1.2	0.791	**1.92%**	0.803	**3.50%**	0.779	**0.33%**
1.4	0.559	**0.10%**	0.546	**-2.36%**	0.546	**-2.38%**

	Sliding Grid		Rotating Domain		Rotating Reference Frame	
J	η_O	$\Delta \eta_O$	η_O	$\Delta \eta_O$	η_O	$\Delta \eta_O$
0.6	0.414	**-3.66%**	0.410	**-4.63%**	0.415	**-3.43%**
0.8	0.527	**-4.44%**	0.521	**-5.44%**	0.528	**-4.15%**
1.0	0.616	**-5.59%**	0.609	**-6.62%**	0.617	**-5.34%**
1.2	0.669	**-7.82%**	0.661	**-8.91%**	0.670	**-7.69%**
1.4	0.663	**-11.44%**	0.662	**-11.59%**	0.662	**-11.59%**

Table 3.5: Open water simulation result of different methods

General view, compared to experiment data, the simulation results of three methods are good at J = 0.6; 0.8 and 1.0, particularly, from 3% to 6% difference for all K_T , K_Q, and η_O . The result of K_Q is also good for all J, less than 5%. The difference just gets higher for K_T at J = 1.2 and 1.4, up to 7% and 13%, respectively. The reason for that could be because the magnitude of K_T is getting very small with increasing J.

Generally speaking, there is not really much difference in terms of numerical result among 3 methods. The Rotating Reference Frame method shows very good estimation of K_Q, giving the best result compared to two other methods. For K_T, the Sliding Grid is the most close to experiment.

To conclude, in terms of accuracy, the result obtained from 3 methods are acceptable: very good estimation of K_Q: lower than 5%, but quite under estimation for K_T at high J: = 1.2 and 1.4. The percentage difference compared to experiment increases corresponding with the decrease of K_T; and the reason, as stated above, could be explained by the magnitude of K_T gets smaller when J is higher.

In terms of computational time, the simulation for all 3 methods is performed in parallel with 16 cores. The average computational time is follows:

Method	Sliding Grid	Rotating Reference Frame	Rotating Domain
Computational time (average)	3500 min = 58.3 h	900 min = 15 h	2400 min = 40h

Table 3.6: Average computational time for each methods

It is clear that Rotating Reference Frame takes least computational time, by less than one-third compared to two other methods. Therefore, Rotating Reference Frame method has big advantage in practical and daily use.

One more factor needs to be concerned to compare 3 methods is the convergence of result. Here, we look at the deviation of thrust and torque in 1 round calculation (last 500 time step for Sliding Grid, 125 and 10 for Rotating Domain and Rotating reference frame) for smallest and biggest J: J = 0.6 and J = 1.4. As can be seen from the *Table 3.7,* the maximum deviation goes for Sliding Grid method with around 2%, and the lowest deviation is obtained by Rotating Reference Frame methods, just only 0.002%. This means that, Rotating Reference Frame methods show very good convergence result.

Sliding Grid							
	J = 0.6				J = 1.4		
	Thrust		Torque		Thrust		Torque	
		Deviation		Deviation				
Max	570.154	**3.109%**	32.7583	**2.82%**	148.139	**1.397%**	12.274	**0.894%**
Min	535.777	**-3.108%**	30.963	**-2.81%**	143.689	**-1.649%**	12.384	**-1.047%**
Average	552.961		31.859		146.098		12.146	
Rotating Domain							
	J = 0.6				J = 1.4		
	Thrust		Torque		Thrust		Torque	
		Deviation		Deviation				
Max	552.5876	**0.034%**	32.16915	**0.037%**	142.273	**0.007%**	11.973	**0.004%**
Min	552.7741	**-0.027%**	32.18091	**-0.026%**	142.282	**-0.006%**	11.974	**-0.003%**
Average	552.4368		32.16084		142.265		12.146	
Rotating Reference Frame							
	J = 0.6				J = 1.4		
	Thrust		Torque		Thrust		Torque	
		Deviation		Deviation				
Max	546.479	**0.0004%**	31.4165	**0.0004%**	138.7954	**0.002%**	11.674434	**0.002%**
Min	546.482	**-0.0007%**	31.4167	**-0.0008%**	138.7985	**-0.004%**	11.67471	**-0.002%**
Average	552.961		31.859		138.7904		12.146	

Table 3.7: Thrust and Torque deviation for each methods

Concerning post processing of result, there is a difference between Sliding Grid and two other methods in Vortex identification. *Figure 3.10* shows the vortex identification based on λ_2 criterion, with λ_2 = -50 for J =1.4. The tip vortex which is captured by Sliding Grid method is clearer and more detailed. The λ_2 (lambda 2) criterion [10] is a common method used to determine vortex. The idea of λ_2 criterion is calculating the symmetric (S) and anti-symmetric (Ω) parts of gradient of velocity vector $\vec{u}$. If we call tensor $J = \nabla u$, then

$$S = \frac{1}{2(J + J^T)} \ and \ \Omega = \frac{1}{2(J - J^T)}$$. After that, 3 eigenvalues of the tensor $S^2 + \Omega^2$ are calculated

and ordered as $\lambda_1 \geq \lambda_2 \geq \lambda_3$. So, the vortex identification is described as follows: if the investigation point is a part of vortex, eigenvalues λ_2 must be lower than 0. In our case, we chose λ_2 = -50.
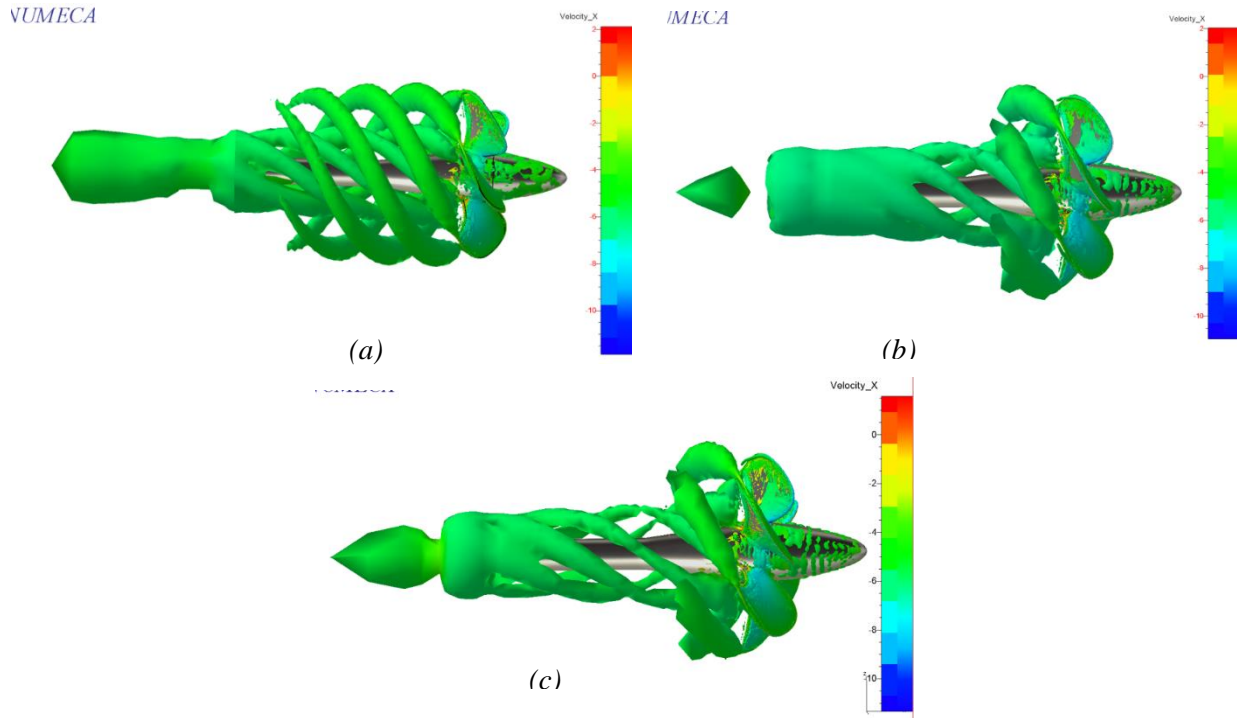
*Figure 3.10: Vortex identification, $\lambda_2 = -50$; J =1.4 for Sliding Grid (a),
Rotating Domain (b), Rotating Reference Frame(c)*

In conclusion, considering 3 main factors: accuracy, computational time and convergence, the Rotating Reference Frame method is the most suitable one for open water simulation by ISIS-solver. Therefore, this method will be used to do open water simulation on the rest content of the thesis.

3.3.3. Comparison of turbulence model

The comparison is carried out by using Rotating Reference Frame method with the mesh size of 3.9 million cells for J =0.6 and 1.4. The turbulence models are: k-ω SST, k-ω BSL, k − ε (Launder − Sharma) and Explicit Algebraic Stress Models (EASM).

Table 3.8 and 3.9 show the numerical result of simulation, and *Figure 3.11* illustrates the comparison among 4 turbulence models in relation with experiment result. At the first glance, it is easy to recognize that k-ε gives worst result, with very large difference compared to experiment one. For J =0.6, the results of k-ω SST, k-ω BSL and EASM model are quite similar (lower than 5% for K_T, K_Q and η_O), there is not clearly distinction. However, looking at J = 1.4, k-ω BSL is slightly better than k-ω SST model (around 2% closer to experiment for K_T and K_Q); and EASM model even is worse than k-ω SST. Then, to conclude, for open water simulation, k-ω SST and k-ω BSL seem to be the best turbulence model, and k-ω BSL might give better result at high J.

k-ω SST turbulence model									
Va	J	T	Q	K_T	ΔK_T	K_Q	ΔK_Q	η_O	$\Delta \eta_O$
2.25	0.6	546.479	31.417	0.623	**-0.986%**	1.432	**2.528%**	0.415	**-3.426%**
5.25	1.4	142.246	11.971	0.162	**-13.706%**	0.546	**-2.376%**	0.662	**-11.590%**
k-ω BSL turbulence model									
2.25	0.6	545.022	31.424	0.621	**-1.250%**	1.432	**2.552%**	0.414	**-3.706%**
5.25	1.4	146.021	12.302	0.166	**-11.429%**	0.561	**0.310%**	0.661	**-11.686%**
k – ε (Launder – Sharma)									
2.25	0.6	521.299	33.049	0.594	**-5.55%**	1.506	7.86%	0.377	**-12.43%**
5.25	1.4	129.260	13.254	0.147	**-21.58%**	0.604	8.09%	0.543	**-27.44%**
EASM									
2.25	0.6	546.322	31.458	0.622	**-1.01%**	1.434	2.66%	0.415	**-3.58%**
5.25	1.4	137.003	11.621	0.156	**-16.89%**	0.530	-5.23%	0.657	**-12.28%**

Table 3.8: Result of open water simulation with different turbulence model

		kω -SST	Kω-BSL	k-ε	EARSM
	ΔK_T	-0.92%	-1.24%	-5.53%	-1.08%
J = 0.6	ΔK_Q	2.55%	2.55%	7.85%	2.69%
	$\Delta \eta_O$	-3.49%	-3.72%	-12.33%	-3.49%
	ΔK_T	-13.74%	-11.43%	-21.73%	-16.93%
J = 1.4	ΔK_Q	-2.29%	0.31%	8.09%	-5.15%
	$\Delta \eta_O$	-11.58%	-11.68%	-27.47%	-12.25%

Table 3.9: Comparison of numerical result among 4 turbulence model
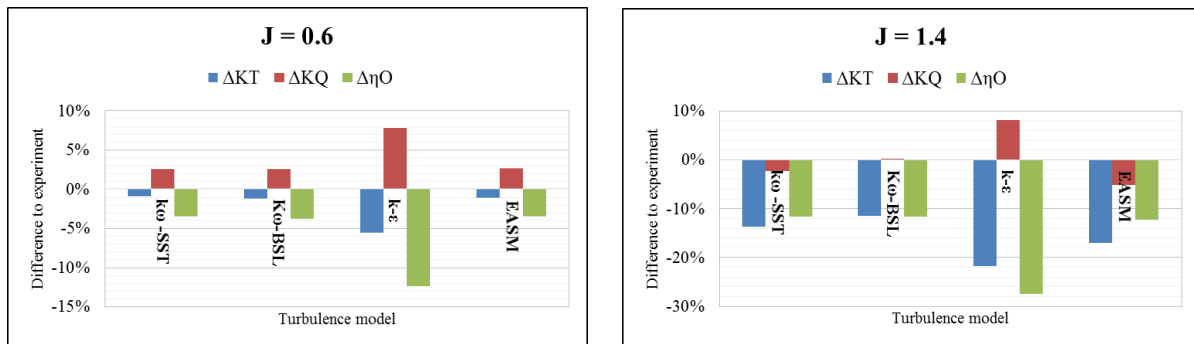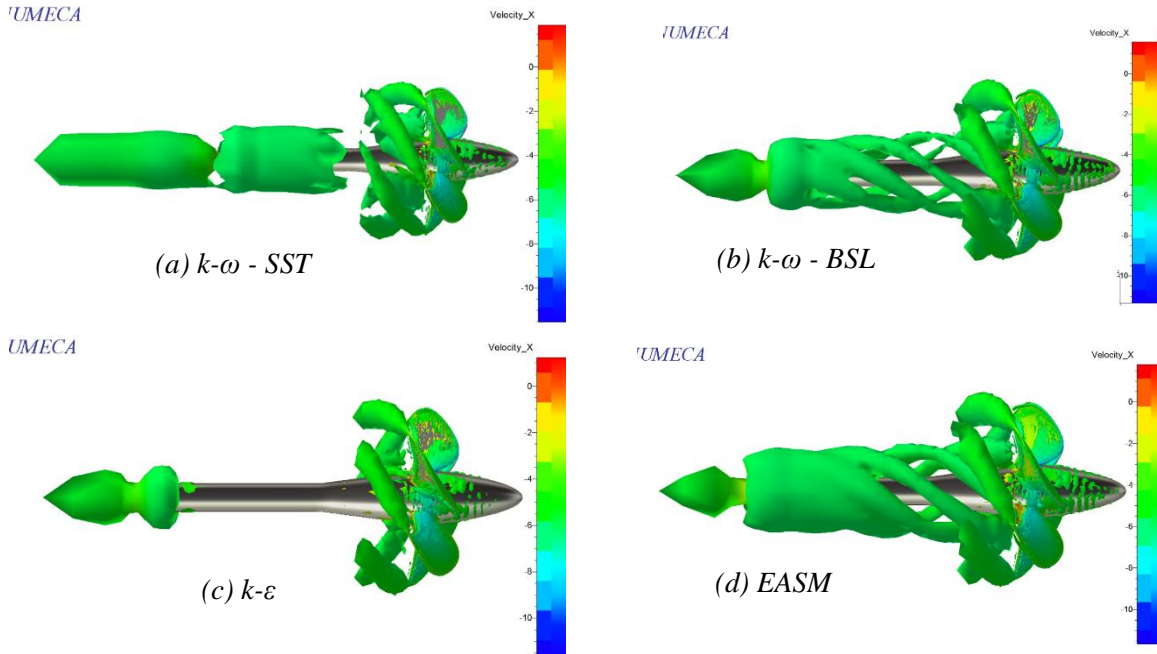

Figure 3.11: Comparison of results among 4 turbulence model J =0.6 (left) and J =1.4 (right)

Vortex distribution is demonstrated by *Figure 3.12*. The tip vortexes in 4 cases are quite similar, but for Hub Vortex, k-ω BSL and EASM seem to be captured better than k-ω SST and k-ε

(a) k-ω - SST

(b) k-ω - BSL

(c) k-ε

(d) EASM

Figure 3.12: Vortex comparison of 4 turbulence model for $\lambda_2 = -50$ and J =1.4

3.3.4. Simulation with laminar flow and high Reynolds number

Currently, in almost simulations of flow around propeller, the flow is assumed as fully turbulence. On the other hand, some experiments show that a large region of laminar flow exist on the propeller. *Figure 3.13* illustrates the laminar flow area which is marked on propeller through the paint test [11]. This test shows that laminar effect appears on large area of propeller at model scale, up to 50-60% of blades area. Some authors also tried performing simulation of propeller with Laminar flow and got some positive result. [12][13]

This can be explained by when doing open water test for propeller at model scale, the low Reynolds number makes the flow rarely fully turbulent. The consequence is that it might lead to the discrepancy between simulation and experiment. That is the reason why the simulation with Laminar flow and high Reynolds number are performed for open water test. For Laminar flow, the solver is setup to use Laminar flow approach instead of turbulence model. In case of high Reynolds number simulation, we increase number of revolution to 100 rpm but still keep the same advance coefficient J by also increasing advance velocity V_A. Turbulence model is used for the case of High Reynolds number is k-ω SST. The Reynolds number in open water

simulation is calculated according to the formula: $Re = \dfrac{c_{0.7}}{v}\sqrt{V_A^2 + (0.7 D\pi n)^2}$, where $c_{0.7}$ is the chord length at 0.7R; V_A is advance velocity and n is revolution. In the case of n = 100rps the Reynolds number is from 5.55×10^6 to 6.34×10^6. The normal (previous) setup with n =15rps, the Reynolds number is from 0.77×10^6 to 0.91×10^6. In 2 cases of simulation, the mesh size is 3.9 million cells, the Rotating reference frame method is selected.
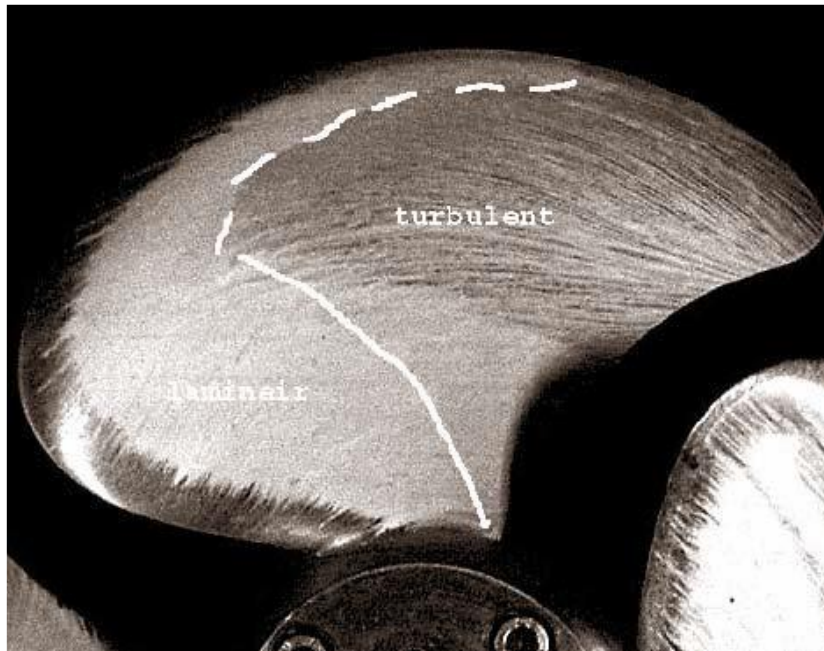
Figure 3.13: Laminar flow area on propeller by using paint test [11]

The result of simulation is presented in *Figure 3.14*. In the over view, two simulations with Laminar flow and Higher Reynolds number give us better result, compared with classical turbulence model : k-ω SST. For all K_T, K_Q, and η_O, the difference with experiment is lower than 5% with Laminar flow – showing very positive estimation. Besides, with high Reynolds number simulation, the result is not improved much, we still observe big distinction in result of K_T compared to experiment for J = 1.4 (around 11%). Though, since the Reynolds number is already quite high (n = 15rps, Re from 0.77×10^6 to 0.91×10^6 and n = 100rps from 5.55×10^6 to 6.34×10^6) – this phenomenon is expected. Furthermore, independent of the Reynolds number, the flow in CFD simulation is always turbulent unless a laminar-turbulent transition is modeled. Then, there is a room to improve the result here by considering laminar – turbulent transition in the simulation. Unfortunately, laminar – turbulent transition model has not been implemented in ISIS – solver.
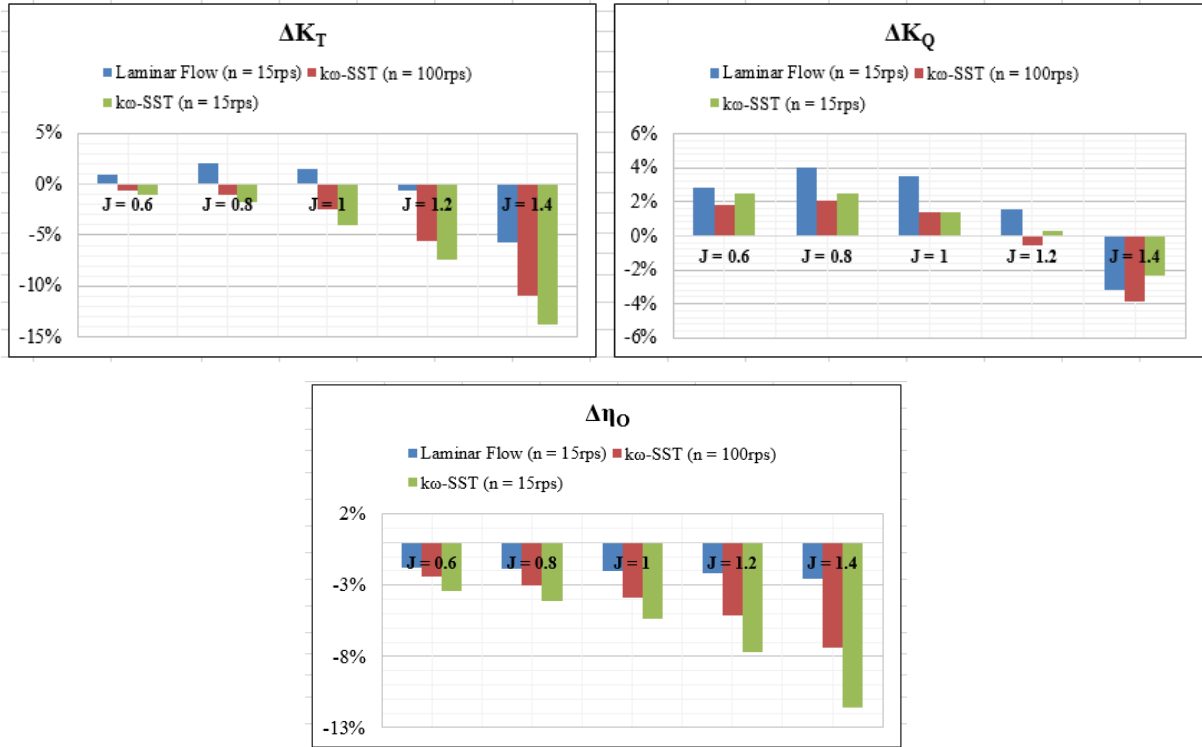
Figure 3.14: Simulation result with Laminar Flow (n = 15rps), k-ω SST (n =100rps) in comparison with experiment result and k-ω SST (n = 15rps)

Advance coefficient	ΔK_T			ΔK_Q			$\Delta \eta_O$		
	Laminar Flow	High Rn number	k-w SST	Laminar Flow	High Rn number	k-w SST	Laminar Flow	High Rn number	k-w SST
J = 0.6	0.96%	-0.59%	-0.99%	2.82%	1.85%	2.53%	-1.81%	-2.39%	-3.43%
J = 0.8	2.10%	-0.97%	-1.74%	4.02%	2.08%	2.52%	-1.84%	-2.99%	-4.15%
J = 1.0	1.45%	-2.52%	-4.08%	3.52%	1.38%	1.35%	-1.99%	-3.84%	-5.34%
J = 1.2	-0.64%	-5.61%	-7.39%	1.58%	-0.52%	0.33%	-2.19%	-5.12%	-7.69%
J = 1.4	-5.64%	-11.01%	-13.71%	-3.18%	-3.87%	-2.38%	-2.52%	-7.41%	-11.59%

Table 3.10: Comparison of result with Laminar Flow (n = 15rps),
k-ω SST (n =100rps) and k-ω SST (n = 15rps)

3.3.5. Assessment and conclusion of result

In previous section, the simulation of open water test for Potsdam propeller test case (PPTC) is carried out with different mesh sizes, methods, turbulence models including laminar flow and higher Reynolds number. Some conclusion can be given as follows:

For mesh convergence study, there is not clearly difference of result between mesh sizes.

Rotating reference frame method proves that it is suitable method for open water simulation, concerning computational time and level of accuracy, as well as convergence of result. The computational time for 3.9 million cells with this method is roughly 15 hours using 16 cores,

less than a half time, compared to 2 other methods. For this reason, it is chosen to do further simulation with different turbulence models. Yet, this method is only suitable for simulation with 1 domain, it means that it cannot be used for simulation of propeller behind the ship. In this case, Sliding Grid approach should be used. The investigation of setup for sliding grid approach in this section is very useful for doing simulation of propeller behind the ship in the next part of thesis.

Turbulence model k-ω SST and, k-ω BSL show that they are best selection for open water simulation. In some case, k-ω BSL model even gives better result for K_T for high advance coefficient J, but the efficiency η_O remains similarly between two turbulence models.

Result of simulation with classical turbulence models is good for lower J = 0.6, 0.8 and 1.0 (less than 6% comparing with experiment for all K_T, K_Q, η_O). However, the estimation of K_T is getting worse with increasing of advance coefficient J, leading the under estimation of η_O (because K_Q is still less than 5% difference compared to experiment). The reason for the under estimation of K_T could be because the magnitude of K_T is getting very small when J is increasing.

The quite surprising result is about simulation with Laminar Flow, where quite much better result is obtained. All the values of K_T, K_Q, η_O, are less than 6% difference with experiment. Increasing Reynolds number also improves result a little. Therefore, these results prove that there is large area of laminar flow on propeller during open water simulation. This phenomenon was also proved by some authors [12] [13]. To validate this result one more time, the next part, we will do the simulation with second test case. This second propeller has small blade areas ratio, it means the Reynolds number might be small. Hence, the simulation with Laminar flow should be performed.

Figure 3.15 presents some post processing result of y^+, axial velocity field and pressure distribution on propeller with Rotating reference frame method and 3.9-million-cells –mesh, J = 0.6 (the result of J = 0.6 is most close to experiment in all simulation). Note that $y^+$is less than 1, but wall function is still used in simulation because ISIS-solver automatically select wall function approach or low y^+ approach.
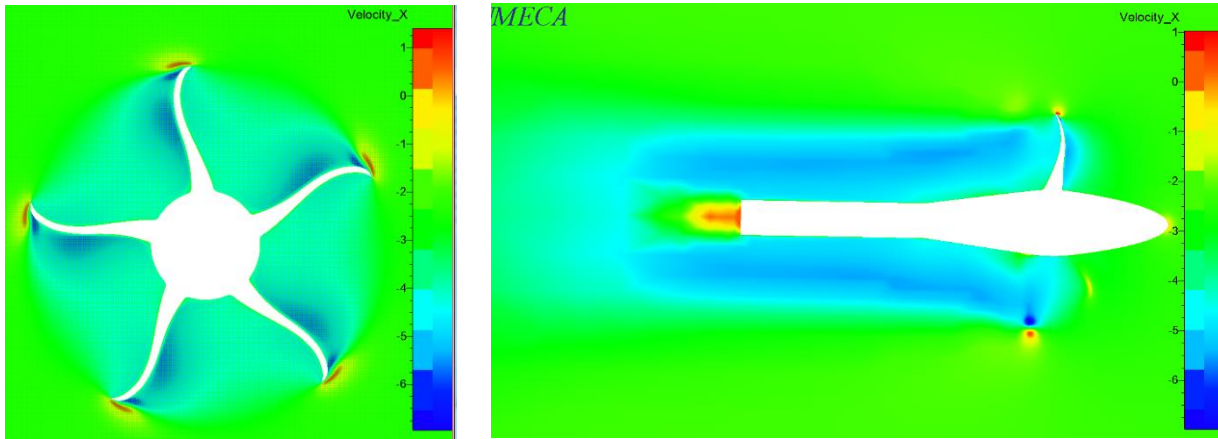
(a): Axial velocity at x = 0 (left) and y = 0(right)
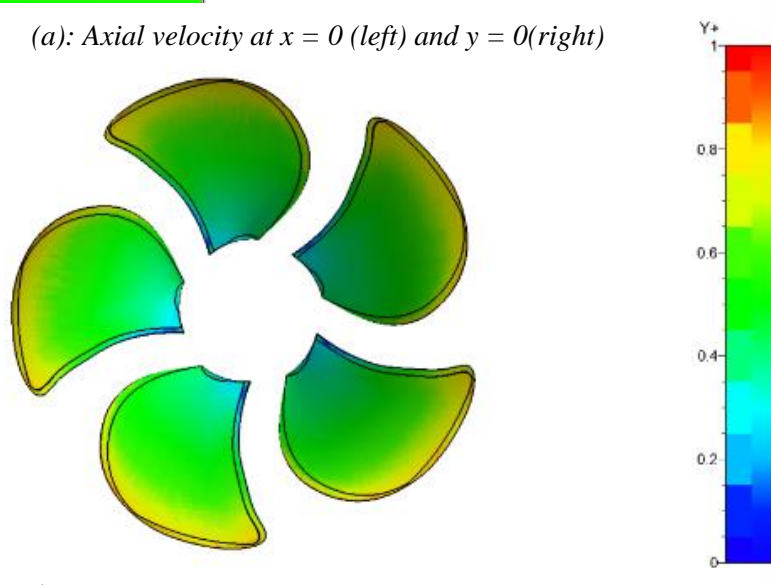
(b): y^+ distribution on pressure side (all smaller than 1)
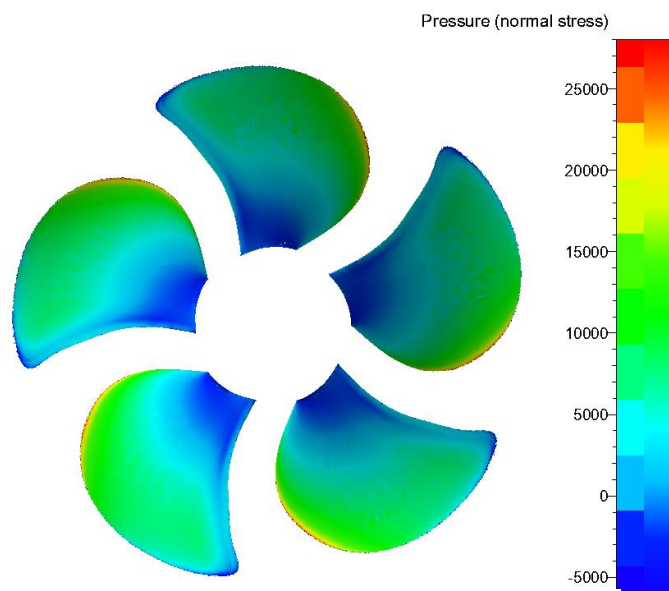
(c): Pressure distribution on pressure side

Figure 3.15: Post processing result for J = 0.6, Rotating Reference Frame method, 3.9 – million – cells mesh

3.4. Second open water test case

The propeller used in the second open water test case is 4-blade propeller. This comes from a part of project in DNVGL, Potsdam. As previous test case, the experimental data for this propeller is available from HSVA. There are CFD result which is provided from "external consultant". In this section, we will carry open water simulation by ISIS – solver by using Rotating reference frame method, with k-ω SST turbulence model. Moreover, as stated above, the laminar flow and high Reynolds number simulation are going to be tested.

The propeller shape is described in *Figure 3.16* below

Figure 3.16: Geometry of second test case propeller
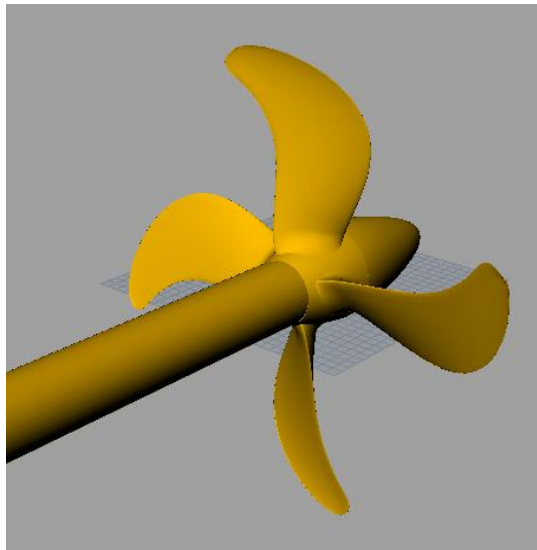
This is a propeller with 4 blades and right hand rotation. Diameter for model scale (D) is 0.2333m, expanded blade area ratio is 0.3766. There are only provided geometry of blades and hub, the Cap and shaft are modelled in Rhinoceros. The shaft is put downstream of propeller to avoid influence of turbulence flow coming to propeller (same as first test case).

There is only 1 mesh to generate with 3.9 million cells. *Figure 3.17* shows the mesh on propeller: high level of refinement at edges and lower number of cells at other areas.

Rotating Reference Frame method is used with k-ω SST turbulence model and Laminar flow. The propeller revolution is set constantly by 18 round per second (rps) – same as experimental test; advance coefficient J is varied by changing advance velocity V_A. Generally, all the setup is similar with the first test case. For higher Reynolds number simulation, number of revolution is increased to n =100rps corresponding with advance velocity V_A to maintain J; turbulence model is still k-ω SST.
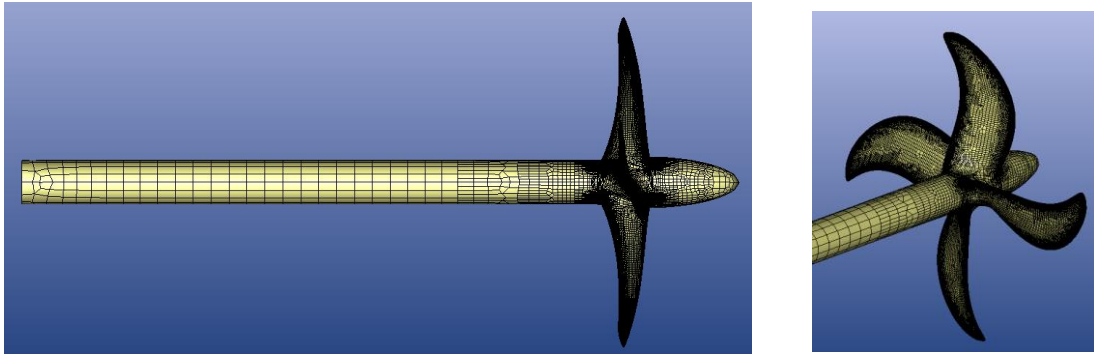
Figure 3.17: Mesh generation for second open water test case

The result of simulation is shown by plotting open water curve in *Figure 3.18.* At first glance, it is clear that simulation with Laminar flow and high Reynolds number give us better result than classical turbulence model k-ω SST. *Table 3.11* presents clearly the difference between CFD simulation and experiment: for k-ω SST with normal revolution, 6% to more than 10% difference is reached. But looking at two others, the results are improved because the distinction are reduced around 5%, and simulation with Laminar flow is slightly better.
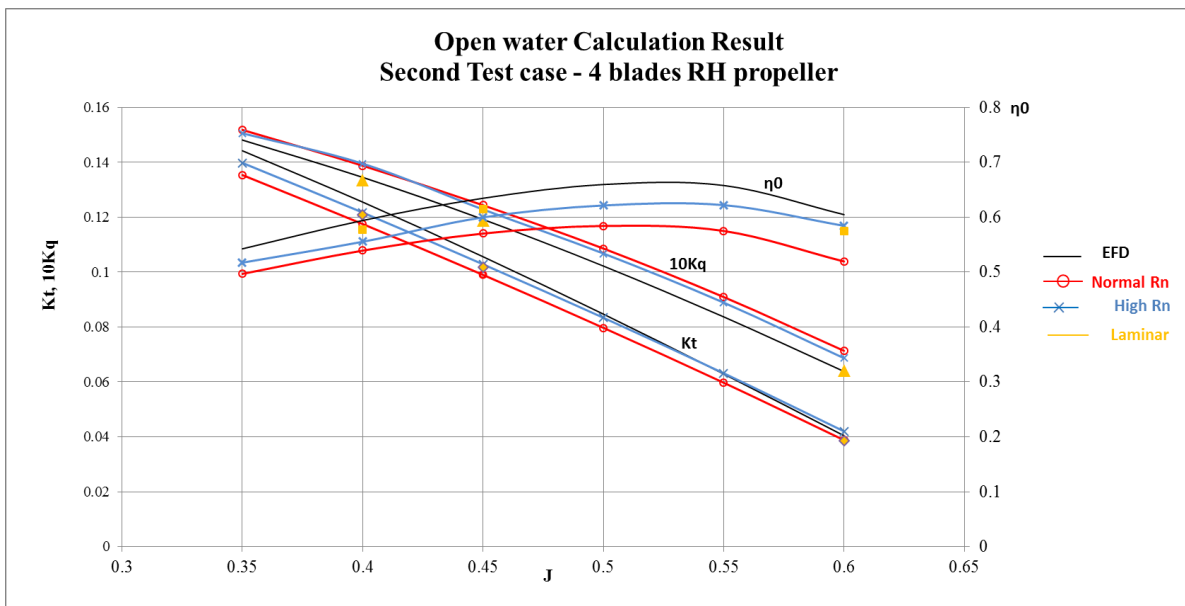
Figure 3.18: Open water curve for second water test case

The result of simulation can be viewed more visually by *Figure 3.19*. By looking at result from "external consutant" , same phenomenom is happened for their simulation: large discrepancy with normal setup, much improvement with Laminar Flow and higher Reynolds number.

	k-ω SST n = 18 rps			k-ω SST n = 100 rps		
J	ΔKt	Δ10KQ	Δη0	ΔKt	Δ10KQ	Δη0
0.35	-6.131%	2.487%	-8.414%	-3.061%	1.654%	-4.643%
0.4	-6.373%	3.160%	-9.238%	-3.038%	3.725%	-6.517%
0.45	-6.253%	4.326%	-10.143%	-2.623%	3.039%	-5.498%
0.5	-5.906%	6.245%	-11.436%	-1.564%	4.483%	-5.787%
0.55	-5.060%	8.631%	-12.601%	0.405%	6.193%	-5.448%
0.6	-3.989%	11.786%	-14.113%	3.971%	7.602%	-3.376%
	Laminar flow n =18rps					
J	ΔKt	Δ10KQ	Δη0			
0.4	-3.737%	-0.828%	-2.930%			
0.45	-3.515%	-0.422%	-3.109%			
0.6	-4.543%	0.529%	-5.047%			

Table 3.11: Result of simulation with second open water test case
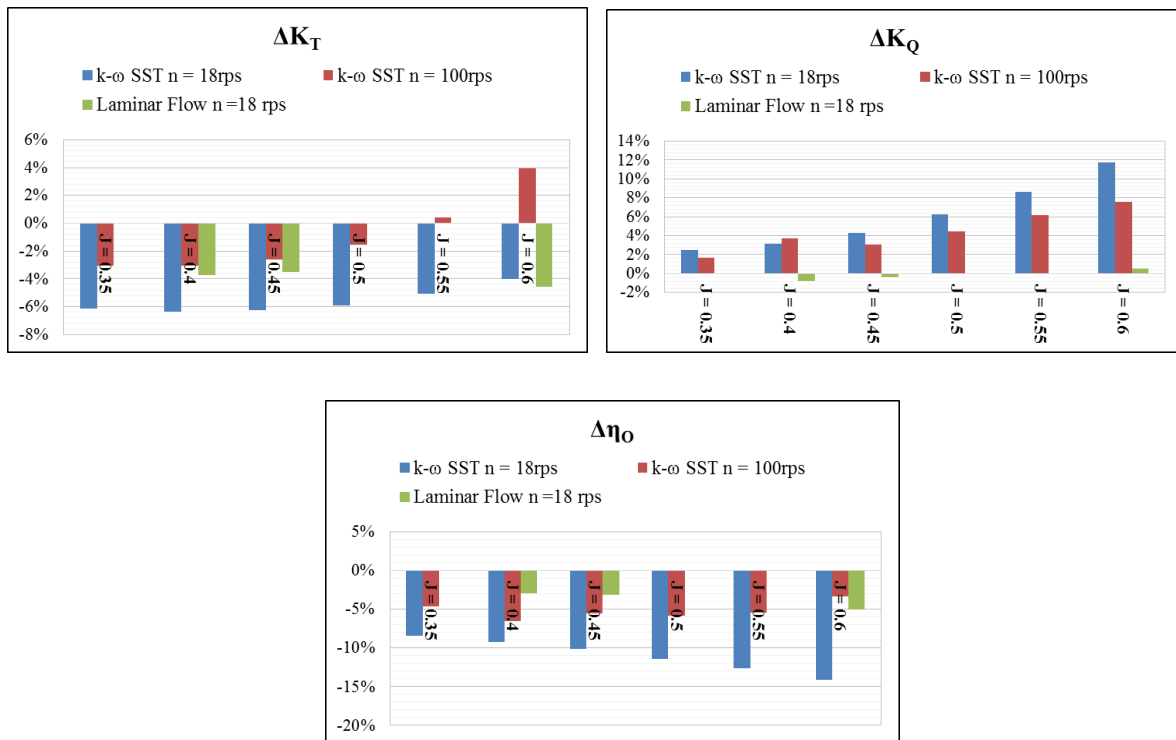
Figure 3.19: Visualization result of simulation with second open water test

3.5. Conclusion

This chapter has presented deep investigation of open water simulation using ISIS solver: from different method, turbulence model to different test case. Generally speaking, acceptable results (difference compared to experiment fluctuates from 2% to around 10%) and less computational time can be obtained with Rotating Reference Frame method and classical turbulence model (k-ω SST, k-ω BSL). Yet, the deviations of simulation are still fairly high for requirements of accuracy. Though, if over a number of test cases, the deviations would be always the same or similar and one could build up reliable correlation. That would be good solution.

Besides, some investigations with Laminar flow and high Reynolds number simulation are carried out and show the improvement in result. It proves that the existence of laminar flow area on propeller, and scales effect in open water test.

The setup and simulation using Sliding Grid method is also studied. It is an elementary step for next part of thesis about simulation of propeller working behind the ship, where rotating reference frame method cannot be applied.

(This page is intentionally left blank)

Master's Thesis developed at the University of Rostock

4. PROPELLER BEHIND SHIP SIMULATION

Simulation and calculation of propeller performance behind the ship (called behind condition) is the second main part of this thesis. When propeller rotates behind the hull form and in the wake field generated by the hull form, the performance of propeller is modified because of the interaction with the hull. Hence, to simulate the characteristic of propeller in behind condition, it is necessary to model full hull form and propeller together. Moreover, because the propulsion experiment is carried out with propeller, ship and rudder (the appendage), to validate the result of CFD simulation verse experiment, the rudder is also need to be modelled. For this reason, it is predictable that the mesh size will have large numbers of cells. As stated in the last chapter, for propulsion simulation, the rotating reference frame method cannot be used, the sliding grid is applied instead.

By modelling full ship and propeller, together with using Sliding Grid method, the time consumption is large. Therefore, firstly, only propeller and hull form are taken part in the simulation; after that, the second step is: adding the dummy rudder into simulation, to assess the influence of rudder. Due to the complexity and time consumption, only one reasonable mesh is created (one mesh for propeller and hull, one other mesh including the rudder).

The ship and propeller geometry which are used to do simulation, are from a Chinese shipyard and they are some parts of a project of DNVGL, Potsdam. The experiment result is provided by China ship scientific research center (CSSRC). The output is wake fraction (w_T), thrust deduction factor (t), relative rotative efficiency (η_R), and hull efficiency (η_H). Besides, the factors that represents performance of propellers also need to be taken into account: thrust coefficient (K_T), torque coefficient (K_Q) (note that these two coefficients are calculated in the case of propeller behind the hull, different from open water case).

In order to get all the output, it is necessary to use open water curve from open water test simulation. Hence, the simulation steps and result of open water for this propeller will be shortly presented. Besides, the experiment result of open water test is provided by CSSRC. We can look at that to study the influence of open water result to propulsion test.

4.1 Ship and propeller geometry

To have consistency with experiment, the simulation is carried at model scale for ship and propeller. The ship is bulk carrier, with a 4-blade propeller. Basic dimension of ship and propeller are described in *Table 4.1* below:

Ship (bulk carrier)		
Length overall	7.5	m
Length between Perpendicular	7.233	m
Breadth moulded	1.0753	m
Design draft	0.4067	m
Displacement	2.708	m^3
Block coefficient C_B	0.855	
Propeller		
Diameter	0.2333	m
Chord length at 0.75R	0.0502	m
Expanded blade ratio	0.3766	
Number of blades	4	
Direction of turning	Right handed	

*Table 4.1: Basic dimension of ship and propeller*
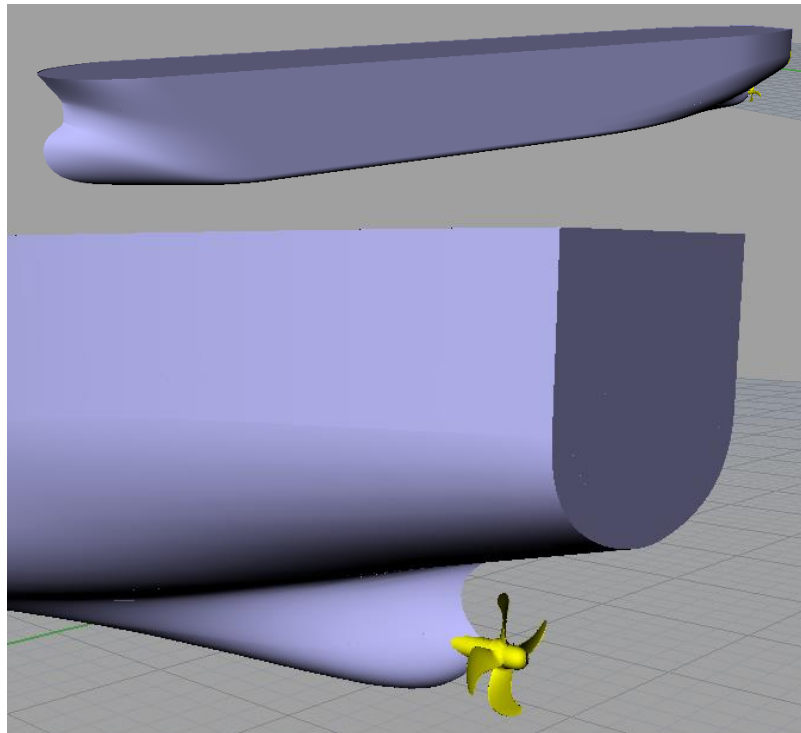
Figure 4.1: 3D geometry of ship and propeller

Master's Thesis developed at the University of Rostock

4.2. Mesh generation

Mesh generation for propulsion test is much more complex than open water test, because full ship and propeller need to be meshed together. Free surface is also meshed. Besides, open water simulation for only propeller need to be carried out. This result will be used at the end of propulsion simulation to determine performance of propeller behind ship. Therefore, two meshes need to be generated: mesh 1 for propeller with ship using Sliding Grid method; mesh 2: only propeller to do open water simulation with Rotating Reference Frame

4.2.1. Mesh generation for propeller behind ship simulation

The mesh contains two domains: ship domain and propeller domain. The sliding interface is created to connect two domains. Ship domain is a box with dimension of 26.25m x 22.5 m x 13.125m (Length x Width x Depth). *Figure 4.2* shows the calculation domain and free surface after meshing step
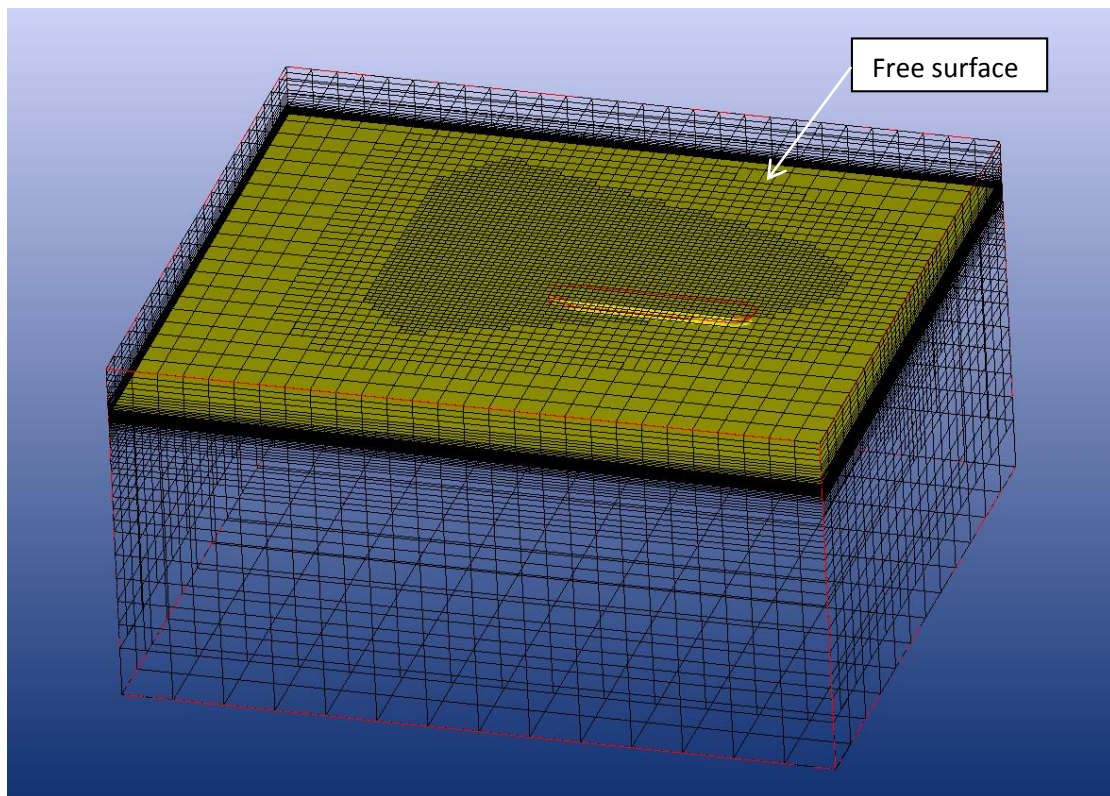
Figure 4.2: Mesh of ship domain and free surface

Free surface and calculation domain are refined at the area close to the ship. For the mesh of ship, whole ship need to be meshed. It is different from resistance simulation, where there is only mesh of half of the ship.

The ship geometry is divided into some "patch", to have different level of refinement for mesh generation: Hull, Hull_coarse, Transom, Transom_Coarse, Shaft, deck, Internal surface (Free surface). The mesh generation step for ship is done almost automatically by using script, developed in DNVGL Potsdam. This script is used for resistance calculation, therefore, some modification is done to adapt to propulsion test. The most important point is that: one cylinder need to be subtracted from calculation domain (the box) to put propeller domain.

The propeller domain is a cylinder, bounding the propeller *(see Figure 4.3).* The same procedure as previous section is applied to mesh propeller. Leading edge, trailing edge is refined with higher level. The detail of refinement is described in *Table 4.2 and Table 4.3*

Name of Patch	Refinement Level	Diffusion
Hull_coarse	5	4
Transom_coarse	5	4
Hull	6	4
Transom	6	4
Shaft	7	4
Free surface_coarse	3	4
Free surface	7	4
Sliding Interface	8	2

Table 4.2: Refinement level for ship domain

Name of Patch	Refinement Level	Diffusion
Leading Edge (curve)	8	4
Trailing Edge (curve)	6	2
Tips (curves)	8	4
Tips (surface)	7	2
Blade (surface)	3	2
Hub (surface)	3	2
Cap (surface)	2	2
Shaft (surface)	2	2
Sliding Interface (surface)	2	2

Table 4.3: Refinement level for propeller domain

The thickness of viscous layer is 0.000417477 for propeller blades and 0.00106738 for propeller and ship, respectively. This leads to expected y^+ higher than 30, then wall function approach is applied in simulation.

The number of cells for Propeller domain and Ship domain are 2.9 and 2.1 million cells, respectively. The total cells are 5 million cells. It can be considered as reason number for mesh size, because time consumption for Sliding Grid is very high.
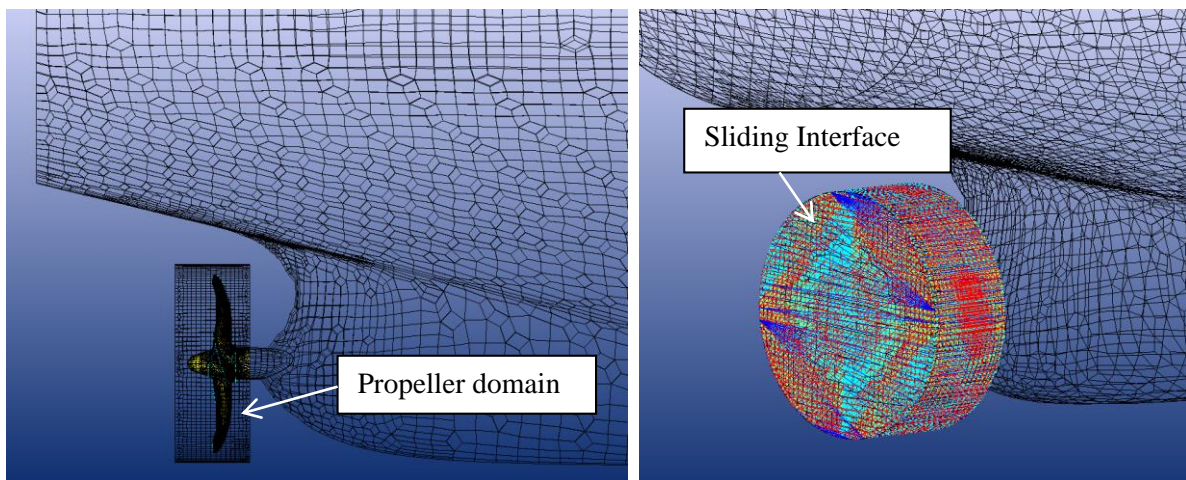
Figure 4.3: Propeller domain and sliding interface
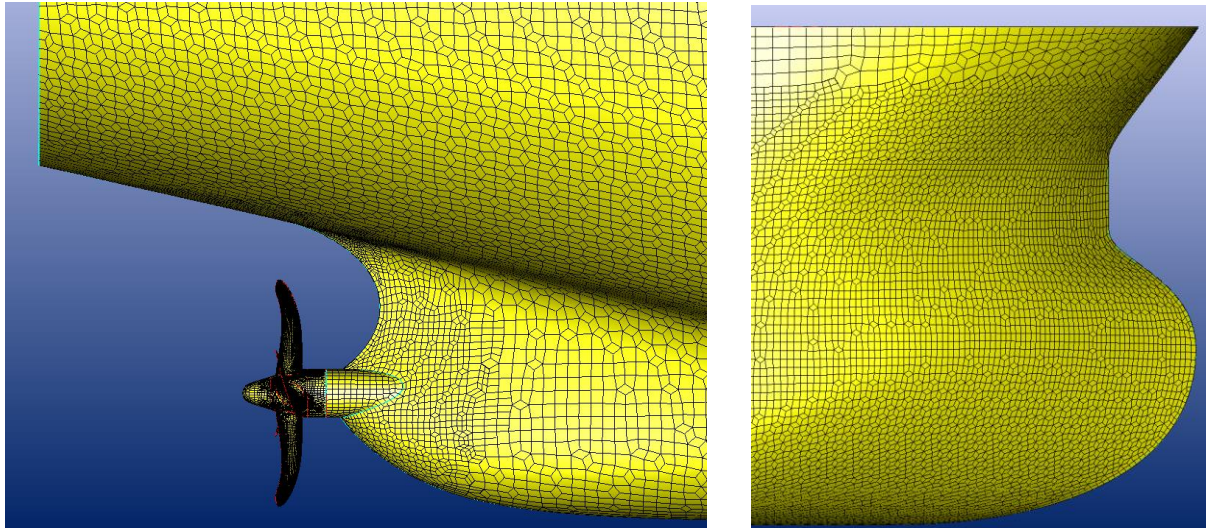
Figure 4.4: Mesh generation of propeller and ship

4.2.2. Mesh generation for open water test

The mesh generation and calculation setup for open water case has been described completely in the previous chapter. Therefore, only brief information about this simulation will be presented.

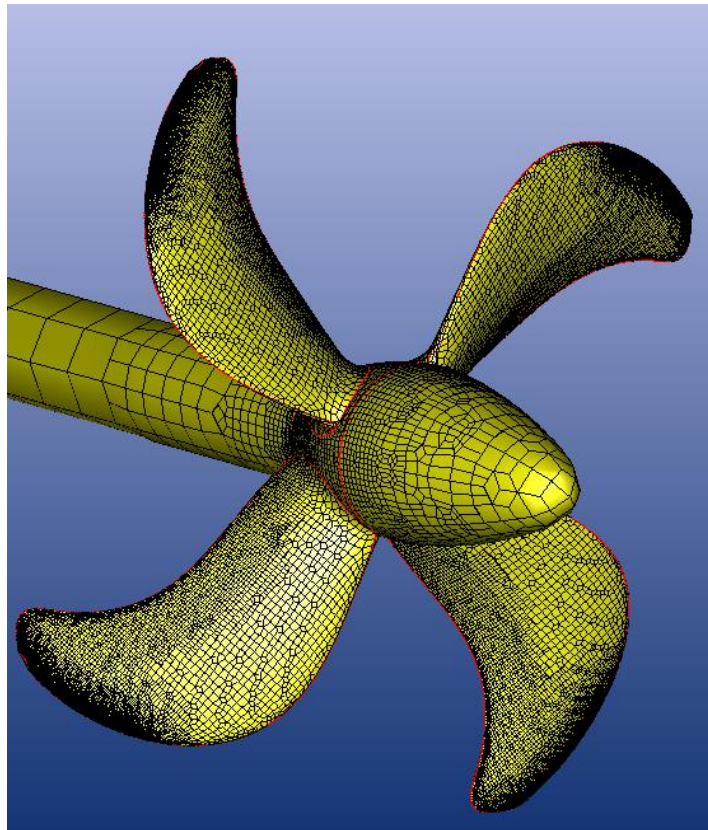There is only 1 mesh is used: 2.1 million cells, using wall function approach, with expected y^+ is 30, to reduce number of cells. Because the main point of this section is about propulsion simulation, only limitation number of cells is generated for open water simulation (*see Figure 4.5*). However, considering the result (presented in next part), this mesh size is acceptable.

Figure 4.5: Mesh generation of propeller in open water simulation using for propulsion calculation

In order to have consistence with propulsion test, turbulence model k-ω SST is used. The simulation is carried out with different advance coefficient J: 0.3, 0.4, 0.5, 0.6, and 0.7 to plot open water curve. This curve is used for interpolation to calculate propeller performance characteristics in the propulsion test.

The experiment data is available from CSSRC. With that data, the interesting thing is that we are not only able to compare experiment result of open water with CFD calculation, but also it is possible to see the influence of open water to result of propulsion test calculation.

4.3. Simulation Setup

This section only describes the setup for propulsion test, detail of open water simulation test is referred in chapter 2.

The simulation is performed at services speed14.5 knots, corresponding with Froude number equals to 0.159. In propulsion test, the equilibrium between propeller thrust and total resistance of the ship (in the self-propeller condition - R_T) need to be established, particularly:

$$R_T = T \text{ (propeller thrust)} + SFC \text{ (skin friction correction)}$$

The skin friction correction force (SFC) is to achieve the theoretically correct propeller loads, taking into account the difference in skin friction coefficients between the model and the full scale ship. This force may be calculated using the ITTC-1957 formula [7]. In the result of experiment, skin friction correction force is already calculated, and therefore, ready to use in simulation.

In order to obtain the equilibrium mentioned above, at least two simulations with different propeller revolution need to be performed, and then interpolate the result. This method also usually uses during self-propulsion experiment test.

The basic setup of simulation is as follows: multi fluid approach (air and fresh water) and free surface. Turbulence model is k-ω SST. For the boundary conditions, wall-function approach is used for solid parts (hull, propeller, shaft, hub and cap), while the external boundary are set to *Far field condition* except *Prescribed pressure* for Top boundary. The propeller is connected to the ship by "Pin" connection.

Each simulation (with one propeller revolution) needs to run two times to reach equilibrium state [14]. The first time, the propeller and ship are accelerated to maximum revolution and speed. The accelerated time is set up to 16 second with "1/4 sinusoidal ramp" profiles (*see Figure 4.6*).
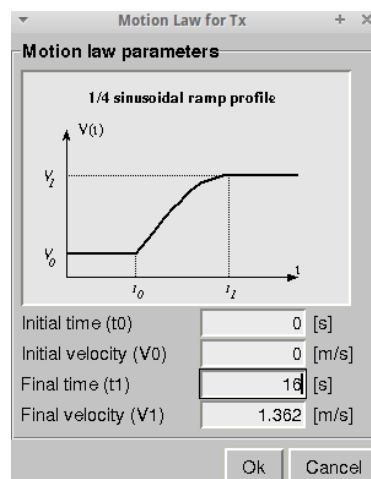

Figure 4.6: Motion setup for propulsion test

It means that the velocity and revolution increase gradually with sinusoidal shape and reach maximum value after 16 seconds. At this stage, large time step is applied to simulation: $\Delta t = 0.026$ second (equal to 5 times step per propeller revolution). The number of iteration per time step is 4. After the force acting on the ship becomes quite steady (around 1000 time step), we switch to second simulation using previous result, but much smaller time step, $\Delta t = 0.000525$ (250 time steps per propeller revolution), and 8 iterations per time step, to stabilize propeller thrust. These two steps are visualized in *Figure 4.7*. *Table 4.4* shows the detail of simulation setup
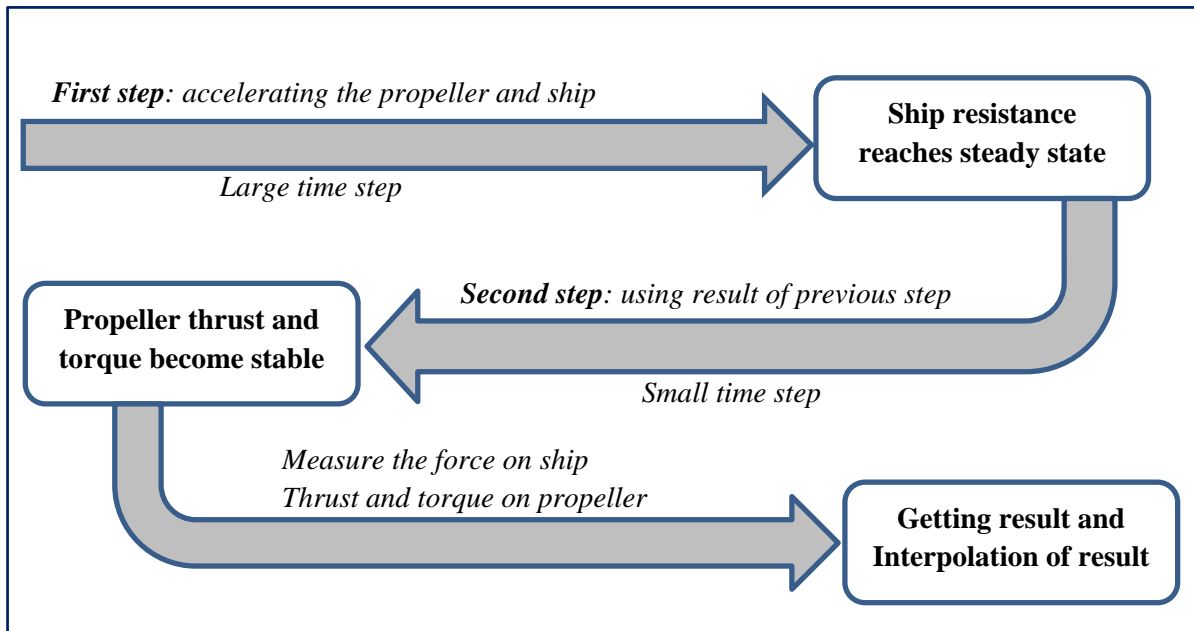
Figure 4.7: Propulsion test simulation steps diagram

Computational case	Propeller revolution (rps)	Time step (s)	
		1st computation	2nd computation
Vs = 14.5knots	7.623	0.026	0.000525
	8.2	0.024	0.000488

Table 4.4: Time steps setup for propulsion test

Two revolutions are selected: 7.623 and 8.2 round per second (rps). After getting result for each revolution, the formulation: $\Delta F = R_T - (T + SFC)$ is calculated. Therefore, if two values

of ΔF are obtained: one positive and one negative, interpolation step could be done to find revolution at which the equilibrium is reached.

4.4. Result of propulsion test simulation

4.4.1. Open water curve

The result of open water simulation for the propeller (which is used in propulsion simulation) is briefly introduced here. Basic setups for this simulation are: mesh with 2.1 million cells, k-ω SST turbulent model and wall function approach. The revolution is fixed, and equal to 18 rps. Advance coefficient J ranges from 0.3 to 0.7. Open water curve and result of simulation in comparison with experiment are presented below:
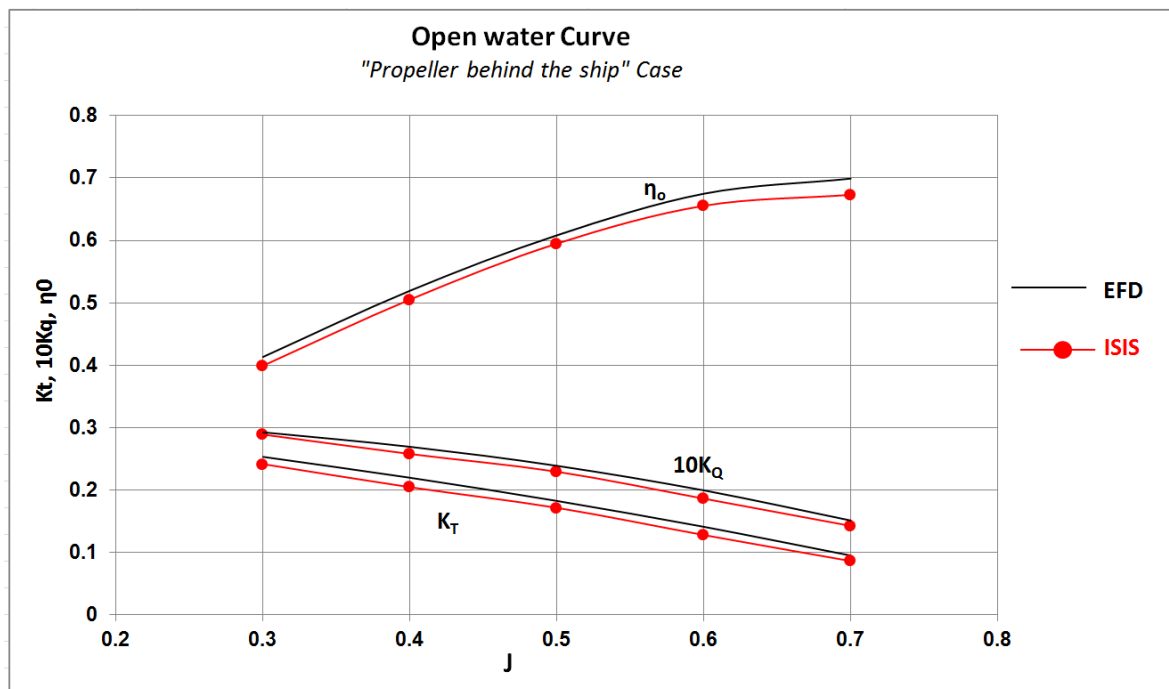
Figure 4.8: Open water curve for Propeller in behind-condition

J	K_T	ΔK_T	K_Q	ΔK_Q	η_o	$\Delta \eta_o$
0.3	0.241	**-4.565%**	0.289	**-1.224%**	0.399	**-3.399%**
0.4	0.204	**-6.907%**	0.258	**-4.298%**	0.505	**-2.721%**
0.5	0.171	**-6.055%**	0.229	**-3.973%**	0.595	**-2.186%**
0.6	0.128	**-9.338%**	0.186	**-6.632%**	0.656	**-2.867%**
0.7	0.086	**-9.288%**	0.142	**-5.735%**	0.673	**-3.722%**

Table 4.5: Result of open water simulation for propeller in behind-condition in comparison with experiment

Overall, the result is good, the difference for open water efficiency is around 3% and torque coefficient is roughly 5%. Thrust coefficient K_T is quite under estimation, reaching 9% for J equals to 0.6 and 0.7. This could be improved by using finer mesh.

4.4.2. Result of simulation for ship without rudder

4.4.2.1. Computational time

Time consumption is a key factor to evaluate the practical use of a method. From the beginning, it is predicted that propulsion simulation with sliding grid is highly time consumption, or in other way, high computational resources. The table below (*Table 4.6*) illustrates the average computational time by using 16 cores on 1 node, the mesh size is 5 million cells:

	Computational time
First computation (large time step)	1200 min = 20 hours
Second computation (small time step)	10000 min = 167 hours = 7 days

Table 4.6: Computational time for propulsion test with Sliding Grid method
(performed in parallel by 16 cores on 1 node)

There is extremely time consumption for second computation; it takes 160s to calculate 1 time step. However, there is a solution for that. The computational time will reduce much if we run parallel on 96 cores over 3 nodes. It only takes around 70 second to calculate one time step. It means the speed increases by 2.5 times. And if the calculation is performed in 128 CPU over 4 nodes, the speed can increase by roughly 4 times, around 50 seconds per time step. Therefore, one simulation (including two steps of computation) can be done within 1.5 days (36 hours).

4.4.2.2. Convergence and Oscillation of the result.

As stated above, the simulation is divided into two steps: step one with large time step, to stable force on the hull; the second step with small time step to get convergence of propeller thrust and torque. However, it is similar to the simulation of open water with Sliding Grid, the force on moment acting on propeller continue oscillating in time, around a certain point (*see Figure 4.9*). The period of fluctuation is consistent with rotational speed. Thus, this state could be considered as convergence and the result is obtained by taking average of force in one round (250 time steps). *Figure 4.9* describes force acting on 1 blade when convergence state is reached. At the end of simulation, the force (resistance) on ship, the thrust and torque on propeller (hub and blades) are measured and taken average.
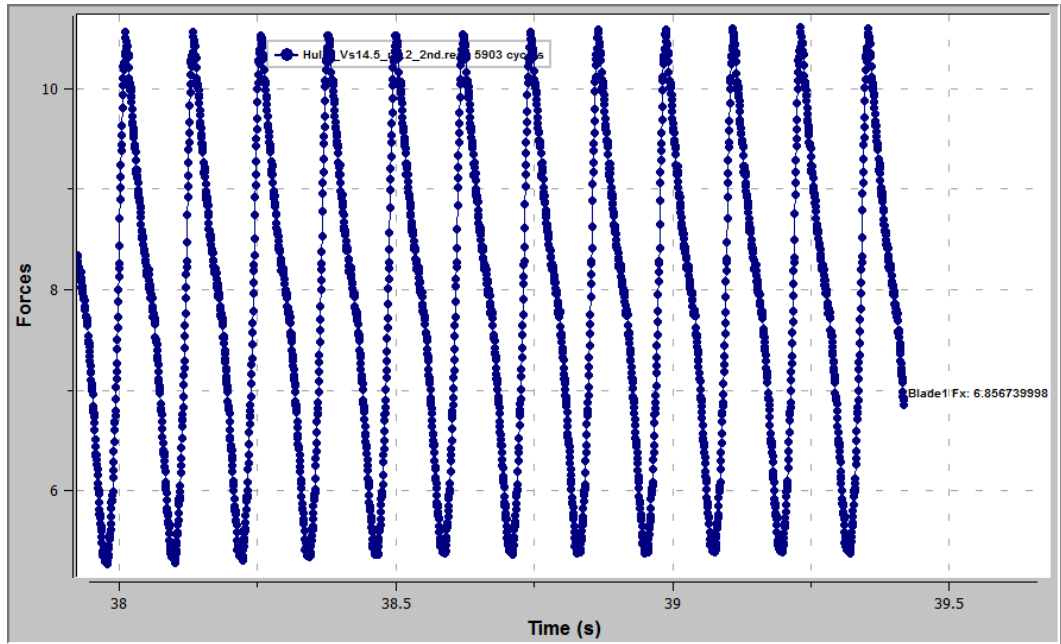
Figure 4.9: Fluctuation of force acting on 1 blade in self - propulsion simulation

4.4.2.3. Result of propulsion simulation without rudder

For propulsion simulation, the equilibrium between ship resistance (in self-propelled condition) and propeller thrust plus skin friction correction. The skin friction correction force (SFC) is already calculated in the experiment: SFC = 20.113N.

We carry two simulations with two different revolution (n): n = 7.623 rps and n = 8.2 rps. For each revolution, the balance $\Delta F = R_T - (T + SFC)$ is calculated, where: R_T is ship resistance in propelled condition, T is propeller thrust. The simulation result and interpolation process is presented as follows (*Table 4.7*):

	Revolution (rps)	R_T (N)	T (N)	SFC (N)	Balance (N)	Torque (Nm)
Calculation	7.623	47.41	25.60	20.113	1.702	0.836
	8.2	48.65	32.03	20.113	-3.496	1.021
Interpolation	**7.812**	**47.82**	**27.71**	**20.113**	**0**	**0.897**

Table 4.7: Result and interpolation for propulsion simulation without rudder

The interpolation shows that 7.812 rps is the revolution at which equilibrium is obtained. The corresponding results are: propeller thrust T = 27.71 N, propeller torque Q = 0.897 Nm. Consequently, the non-dimensional numbers are calculated as follows

Thrust coefficient: $K_T = \dfrac{T}{\rho n^2 D^4} = 0.154$

Torque coefficient: $K_Q = \dfrac{T}{\rho n^2 D^5} = 0.213$

Thrust deduction coefficient: $1 - t = 1 - \dfrac{T - R_{T(tow)} + SFC}{T} = 0.808$

Where $R_{T(tow)}$ = 42.5 N: total resistance of ship in towing condition (the pure resistance test without propeller).This resistance is taken from experiment test, considering that accurate result of pure resistance simulation could be obtained by using ISIS-solver. However, further development might be taking pure resistance test into account, and evaluating the difference by using experiment value or CFD calculation one. The pure resistance simulation is often carried out at DNVGL, Potsdam to validate the performance of hull form after optimization step and the level of accuracy for this kind of simulation is already validated.

To calculate others parameter (propulsion factors: wake coefficient, relative rotative coefficient…), the open water curve (*Figure 4.8*) and thrust identity method are used. The thrust identity method is mentioned in the theory part of this thesis: the thrust is considered as no change, and the toque is extrapolated from open water curve. There are two open water curves in *Figure 4.8:* one is from experiment and the other one is from CFD calculation result. Hence, to see the influence of open water result to propulsion result, we can use both curves from experiment and CFD calculation. Calculation results are presented in *Table 4.8* below

Advance coefficient J and torque coefficient K_{Qo} (in open water condition) are extrapolated from the open water curve using thrust identity method as mentioned above.

Propeller advance speed: $V_A = JnD$

Open water efficiency: $\eta_O = \dfrac{JK_T}{2\pi K_{Qo}}$

Relative rotative efficiency $\eta_R = \dfrac{K_{Qo}}{K_Q}$ where K_{Qo} and K_Q are torque coefficient for open water and propelled condition, respectively

Effective wake coefficient (1 - w): $1 - w = 1 - \dfrac{V_S - V_A}{V_S}$ where V_S and V_A are ship velocity and advance velocity, respectively

Hull efficiency $\eta_H = \dfrac{1-t}{1-w}$

	Using ISIS-CFD open water curve	Using experiment open water curve
Thrust coefficient K_T (thrust identity)	0.154	0.154
Advance coefficient J	0.541	0.569
Propeller advance speed V_A (m/s)	0.986	1.038
K_{Qo} (open water)	0.209	0.211
Open water coefficient η_O	0.633	0.659
Relative rotative efficient η_R	0.980	0.992
Effective wake coefficient (1 - w)	0.724	0.762
Hull efficient η_H	1.116	1.060

Table 4.8: Calculation of propulsion factors

	With open water curve from ISIS		With open water curve from experiment		Experiment result
		Compare to experiment		Compare to experiment	
Thrust coefficient K_T	0.154	-7.49%	0.154	-7.49%	0.166
Torque coefficient K_Q	0.213	-3.14%	0.213	-3.14%	0.22
Revolution n	7.812	2.48%	7.812	2.48%	7.623
Thrust deduction coefficient (1 - t)	0.808	3.06%	0.808	3.06%	0.784
Advance coefficient J	0.5408	-0.04%	0.569	5.26%	0.541
Open water coefficient	0.633	-0.92%	0.659	3.07%	0.639
Relative rotative efficient η_R	0.980	-3.48%	0.992	-2.30%	1.015
Effective wake coefficient (1 - w)	0.724	2.37%	0.762	7.80%	0.707
Hull efficient η_H	1.116	-1.02%	1.060	-6.01%	1.128

Table 4.9: Comparison between CFD calculation and experiment result

Table 4.9 illustrates the comparison between CFD result and experiment. Overall, the result of CFD is good, with the difference from experiment just around 3%, except the under estimation for K_T, the difference for K_T is 7%. It is clear that using open water result from CFD simulation gives quite better estimation of self-propulsion characteristic, than using open water

result from experiment result. Moreover, the result of solving flow in self-propulsion condition seems better than open water condition, even the flow is more complicated to solve. This phenomenon might be explained by "well - combination" of numerical error in two simulations: open water and self-propulsion. It means that the difference error in two simulations neglect each other, then giving pleasant result.

Particularly, in self-propulsion simulation, the thrust coefficient (K_T) is under-estimated by 7.5%. In open water simulation (by ISIS solver), K_T is also under estimated from 5% - 9%. Therefore, using thrust identity method, advance coefficient (J) is determined by only 0.04% difference with experiment. And it leads to good agreement of other factors (open water coefficient, effective wake coefficient) with experiment result. In contrast, if open water curve from experiments is used, the advance coefficient (J) (of self-propulsion simulation) is higher than experiment by 5.2%, leading other propulsion parameters are different from experiment by 3 - 7%.

It is noted that this simulation is performed without rudder, and the experiment is carried out with rudder. Thus, the next part, a dummy rudder is added into the simulation. With the contribution of the rudder, it is expected that the thrust of propeller increases, and the difference in terms of thrust declines.

Before doing the simulation with rudder, another simulation for propeller revolution n = 8rps is carried out, to see the influence of interpolation step to final result. *Table 4.10* presents the interpolation for n = 8rps, in comparison with interpolation for n = 8.2 rps (the previous simulation). There is no significant difference between two interpolations:

	Revolution (rps)	R_T (N)	T (N)	SFC (N)	Balance (N)	Torque (Nm)
Calculation	7.623	47.41	25.60	20.113	1.702	0.836
	8.0	47.69	29.43	20.113	-1.846	1.949
Interpolation	**7.804**	**47.55**	**27.44**	**20.113**	**0**	**0.890**
Previous interpolation	**7.812**	**47.82**	**27.71**	**20.113**	**0**	**0.897**

Table 4.10: Comparison between two interpolations

To visualize the result, some figures below illustrates the post processing step for pressure distribution on propeller, free surface elevation and vortex identification.
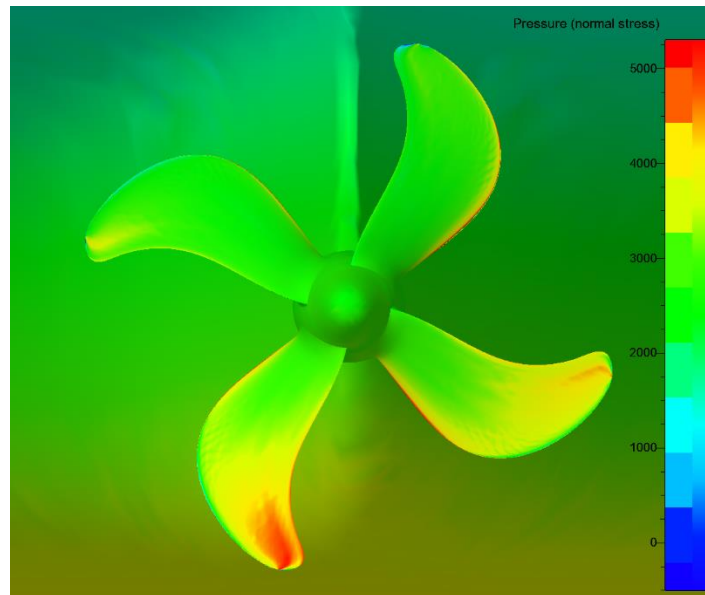
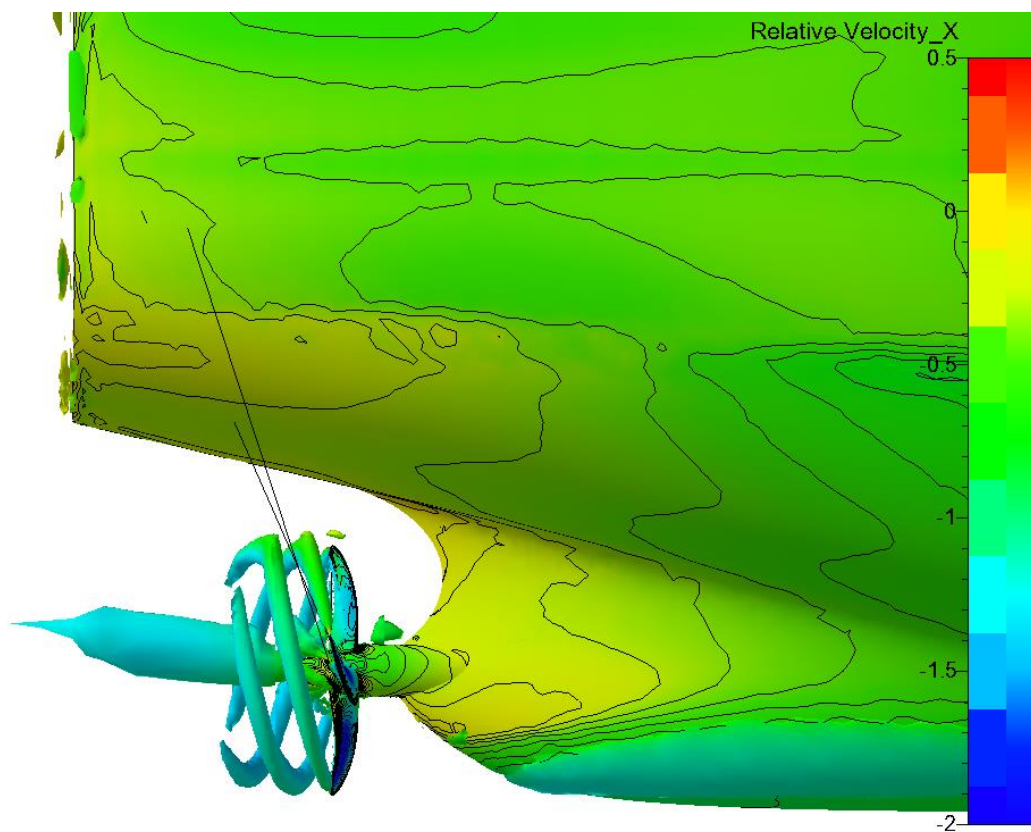*Figure 4.10: Pressure distribution on propeller (Pressure face)*

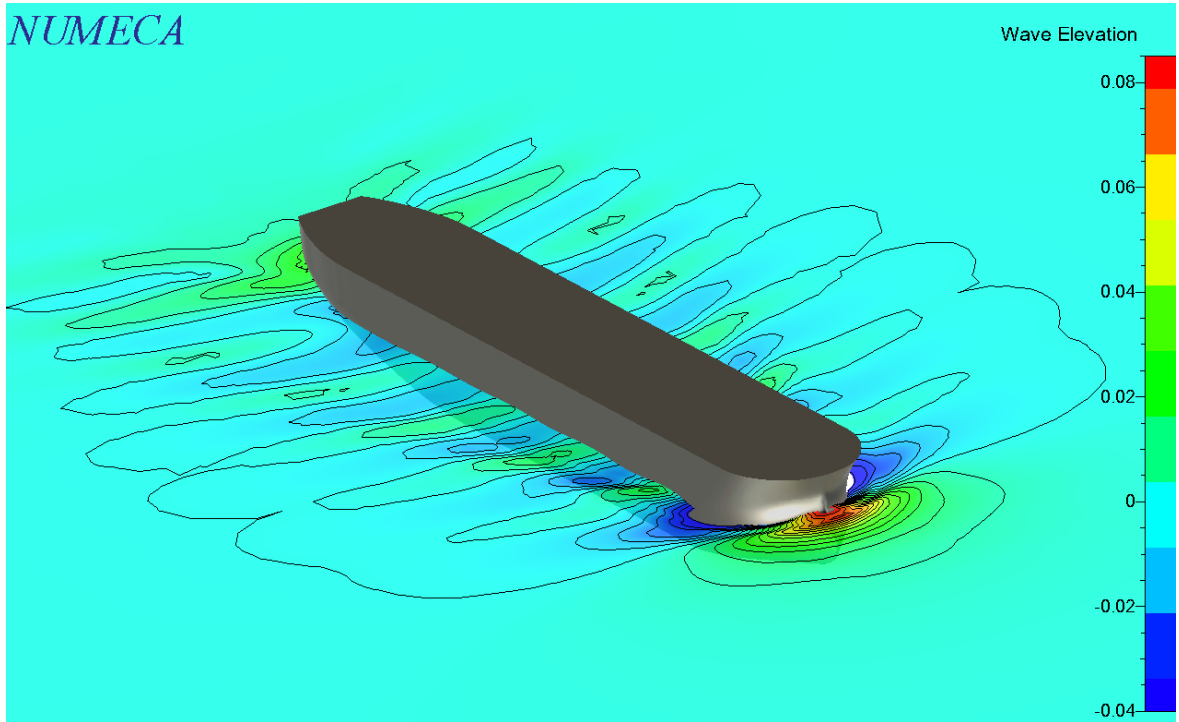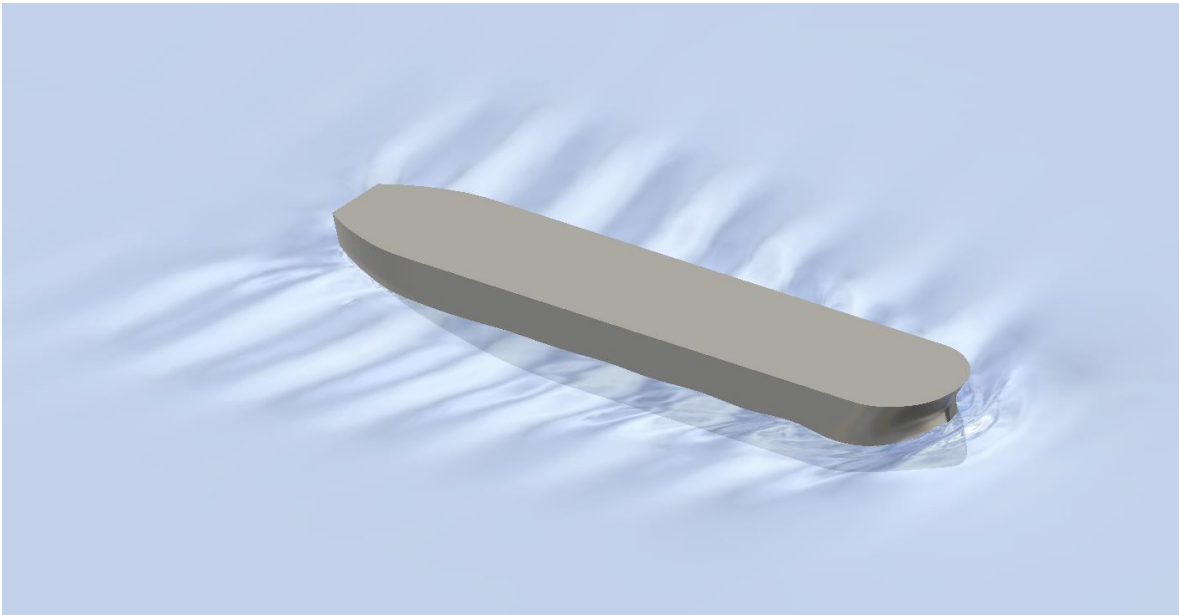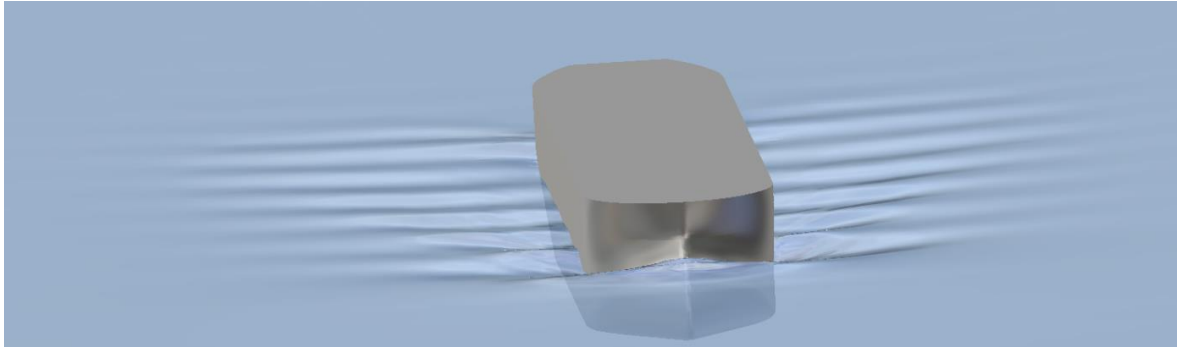*Figure 4.11: Vortex distribution ($\lambda_2 = -50$) and axial velocity distribution at stern*
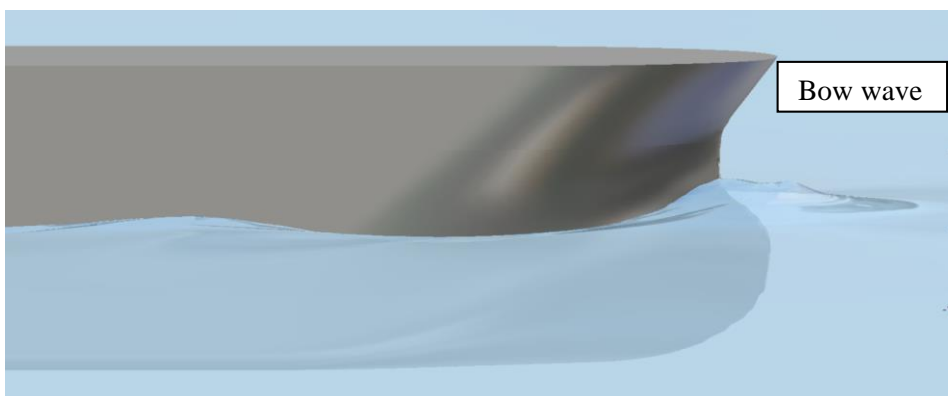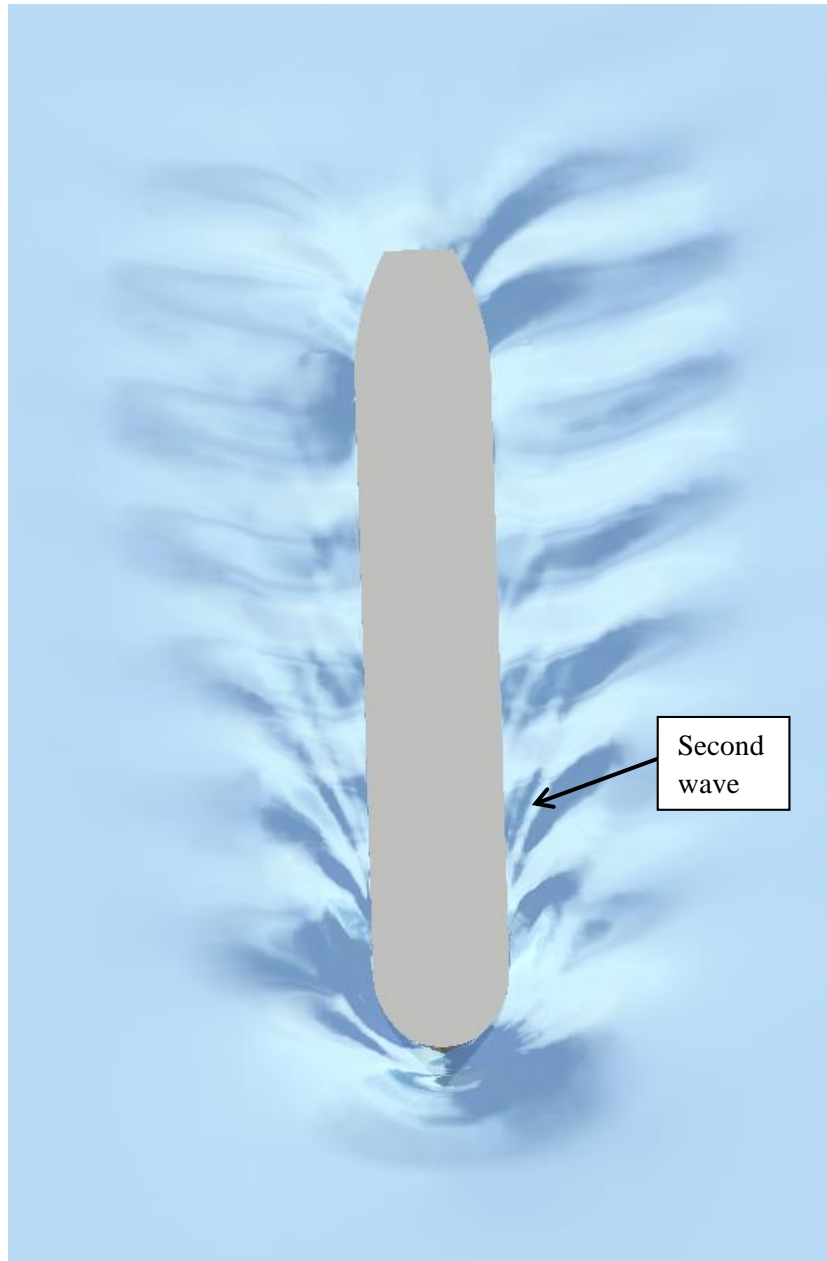
Figure 4.12: Free surface elevation

Figure 4.13: Illustration of wave around ship

Figure 4.10 describes the pressure distribution of propeller, high pressure is noticed at leading edge and blades has deeper position into water. By using λ_2 criterion, tip vortex and hub vortex are expressed in *Figure 4.11*. As mentioned in Open water part, Sliding Grid method can capture vortex well. The wave and free surface elevation are shown in *Figure 4.12 and Figure 4.13*. The free surface is solved quite well, in those pictures, wave is presented clearly. There is higher wave at bow; and it is reasonable.

4.4.3. Result of simulation for ship with dummy rudder

The dummy rudder is added into ship domain. Therefore, the mesh has to be generated. The rudder is created by extrude NACA-18 profile (*Figure 4.14*), then attach with the ship. Dimension of the rudder is shown in *Figure 4.14*
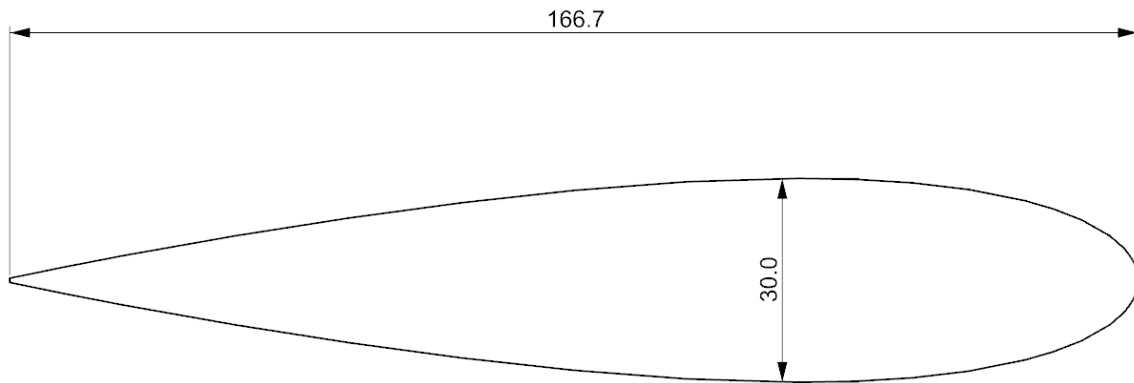
Figure 4.14: Cross section of the rudder

New mesh has 5.095 million cells, with 70.000 cells for rudder. The mesh of rudder is quite coarse, however, it is still sufficient to capture geometry properties. Computational setup is kept the same (services speed $V_S = 14.5$ knots), only mesh is changed.
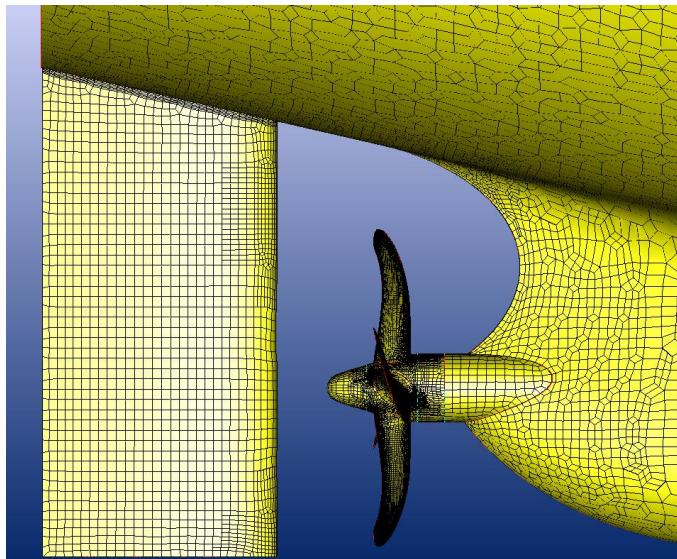

Figure 4.15: Mesh of rudder with ship and propeller

By only increasing 70.000 cells, the computational time is not increased much. However, it still takes more than 48 hours to finish simulation on 96 cores over 3 nodes. This simulation is performed at the end of the internship. Due to high time consumption and computational resources, in this simulation with rudder, there is only one simulation with n = 7.623 (same as experiment result) which is carried out, then comparing with experiment result. The interpolation process is not performed, it means there is an imbalance of ship resistance and propeller thrust. *Table 4.11* illustrates the result with force measured on ship (resistance) and propeller (thrust), in comparison with experiment and the simulation without rudder.

	Revolution (rps)	R_T (N)	T (N)	SFC (N)	Balance (N)	Torque (Nm)
Without rudder	7.623	47.41	25.60	20.113	1.702	0.836
With rudder	7.623	48.97	27.34	20.113	1.52	0.829
Experiment	7.623	48.65	28.55	20.113	0	0.884

Table 4.11: Result of simulation with rudder in comparison with experiment result and without rudder
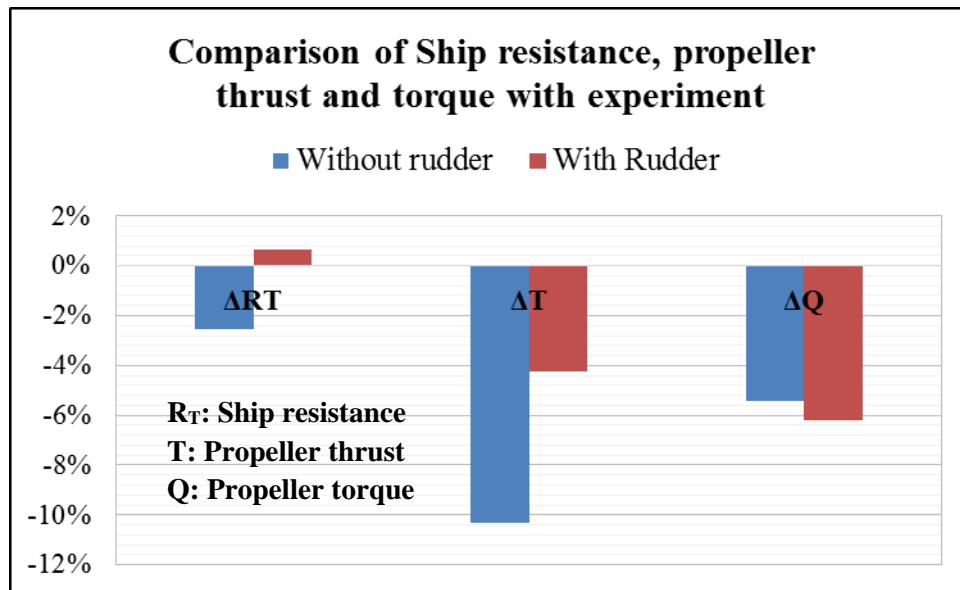
Figure 4.16: Comparison of Ship resistance, propeller thrust and torque with experiment, in case of simulation with and without rudder, n =7.623rps, V_S = 14.5 knots

As expressed in *Figure 4.16*, with the contribution of rudder, the ship resistance (in propelled condition) is very close to experiment (less than 1%, compared to 2.5% without rudder). It is explained by the increasing wetted area, or in other way, there is also the resistance due to rudder.

The thrust of propeller also rises, from 10% without rudder to 4% with rudder. Referring to literature, this phenomenon is called "**rudder blockage**" [15]. When a rudder is placed downstream of a propeller, the rudder will block and separate the flow from propeller, influence the thrust and torque generated by propeller. *A. F. Molland and S. R. Turnock* [15] found out that the relative position of the rudder to propeller *"can have significant influence on the propeller characteristics"* [15]. Besides, *A. Sánchez Caja et al* [16] pointed out that there are two sorts of "rudder blockage" in self-propulsion simulation with rudder. The first one is mentioned above, called "physical blockage". The other one is "numerical or computational blockage". This is the affection of sliding grid method when there is presence of nonphysical change of the inflow, because the domain of propeller rotates in front of the solid, non-rotating part (rudder). *A. Sánchez Caja et al* [16] also carried out different analysis with different relative location of rudder to propeller, to investigate numerical blockage. In their simulation result (*Table 4.12*), the propeller thrust increase up to 20% with the "effective distance" between propeller and rudder: (Note that the simulation is carried out for ducted propeller)

	Without rudder	With rudder
K_T blades	0.145	0.2
K_T blades + duct	0.183	0.235

Table 4.12: Simulation of ducted propeller with and without rudder by other authors [16]

They showed that there are changes in pressure distributions between the computations made without and with rudder; leading to the increase of thrust. This result was also investigated by *Vladimir Krasilnikov et al* [17]. Coming back to the simulation in this thesis, different components of forces (pressure and viscous force) acting on propeller are analyzed in *Table 4.13* below:

Forces	With rudder			Without rudder	
	Blades	Hub	Rudder	Blades	Hub
Pressure force - Fxp (N)	26.22	1.58	0.58	24.70	1.54
Viscos force - Fxv (N)	- 0.46	- 0.01	0.60	- 0.46	- 0.01
Total force - Fx (N)	25.77	1.58	1.18	24.24	1.53

Table 4.13:: Decomposition of forces acting on propeller

It can be seen that there is the increase of pressure force on blades in case of simulation with rudder (from 24.7N to 26.22N). It could be due to the "rudder blockage" phenomenon, leading to the increase of the pressure differences between pressure side and suction side of blades.

Consequently, the thrust rises by around 6%. *Figure 4.17* shows the pressure field in the stern area.

Regarding propeller torque, no much difference can be seen with the presence of rudder.

To conclude, the contribution of rudder is in terms of "rudder blockage" aspect. It also depends on relative location of rudder to propeller [15][16][17]. Moreover, Sliding Grid method influences the result by a so-called "numerical blockage" [16]. It makes the simulation result is closer to experiment: less than 1% for ship resistance and 4% for propeller thrust, compared with 2.5% and 10% respectively in case of no rudder.

Please note that, in two cases of simulation with and without rudder, the results are *compared with the experiment which is performed with rudder*. Therefore, the simulation with rudder gives better result is reasonable. The reason for doing two cases of simulation (with and without rudder) is investigation of the influence of rudder to propulsion test. If the influence can be neglectable, the mesh size can be reduced by not meshing rudder. However, the study here points out the affection of rudder to propulsion test. It is necessary to include rudder in self-propulsion simulation to get more accuracy result
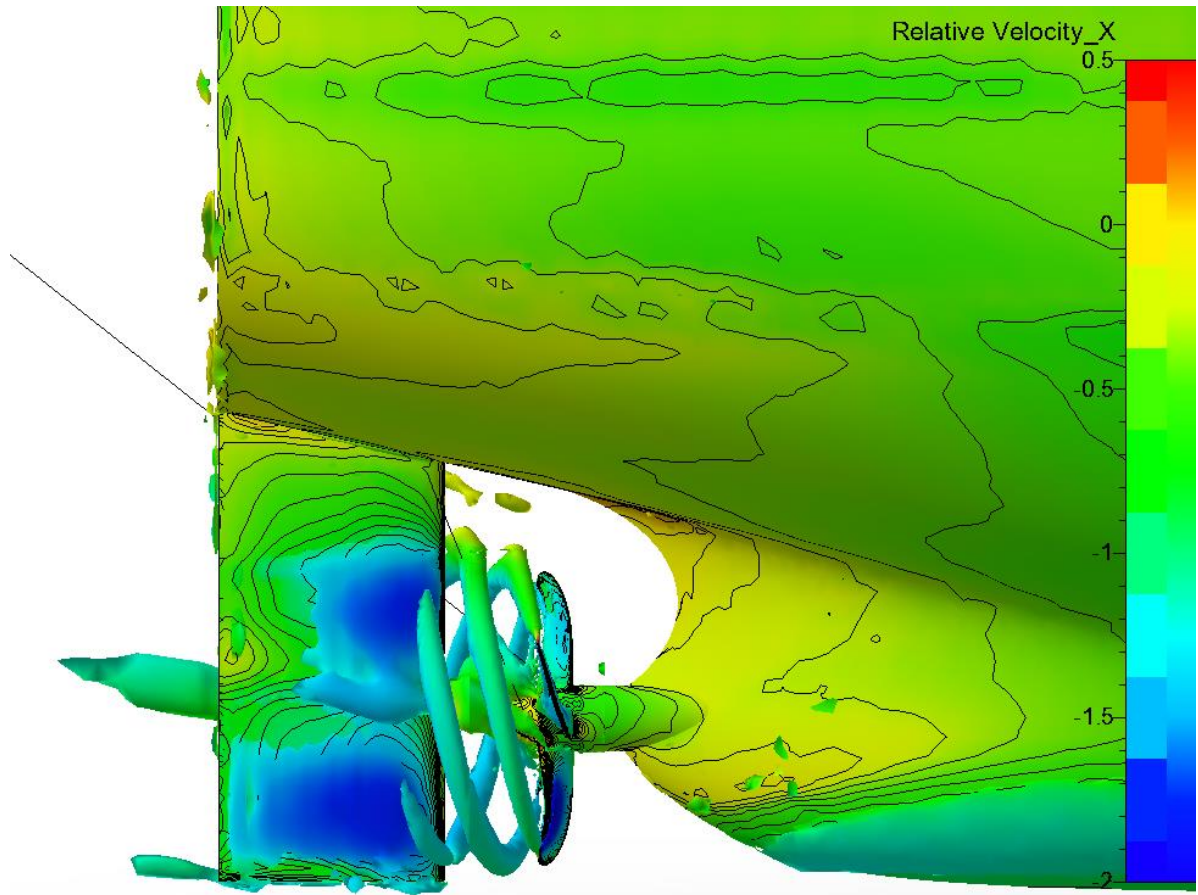
In post-processing process, the pressure distribution, vortex identification and stream line are visualized. The vortex is identified by using λ_2-criterion with $\lambda_2 = -50$.
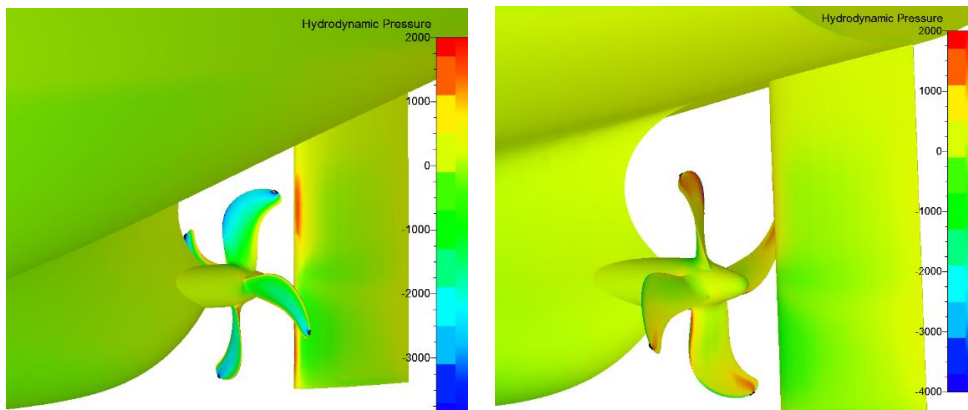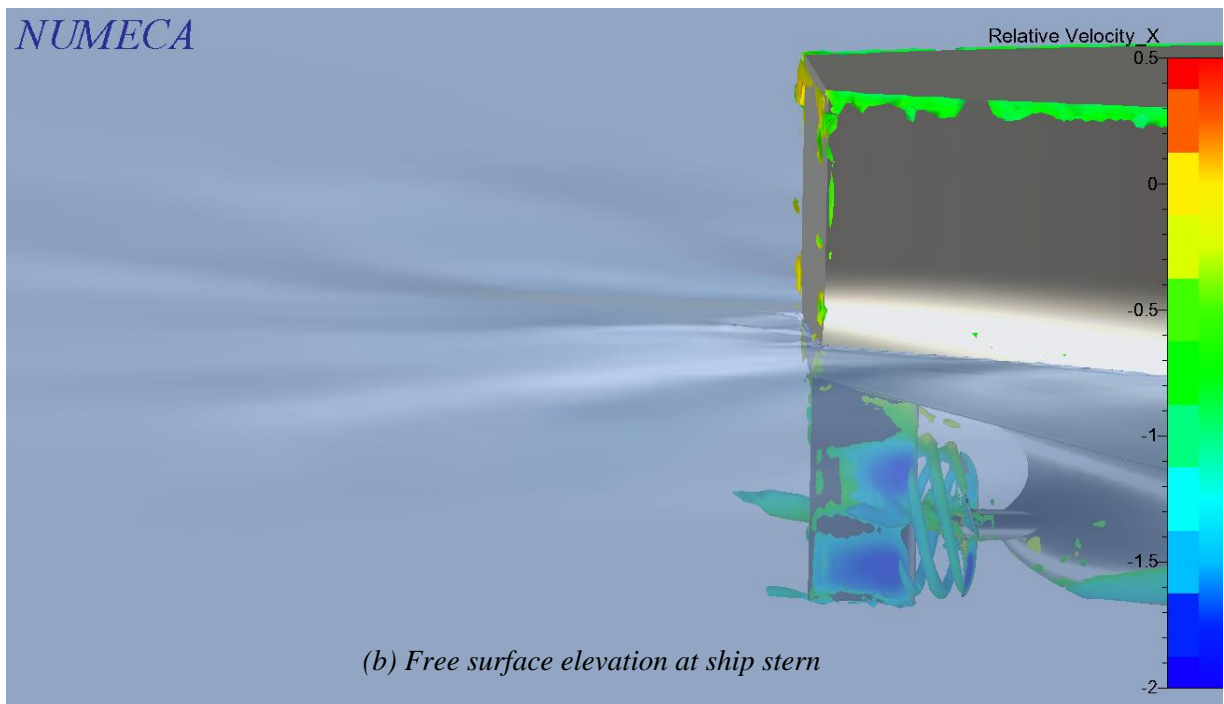

Figure 4.17: Hydrodynamic pressure distribution on stern of ship in the simulation with rudder
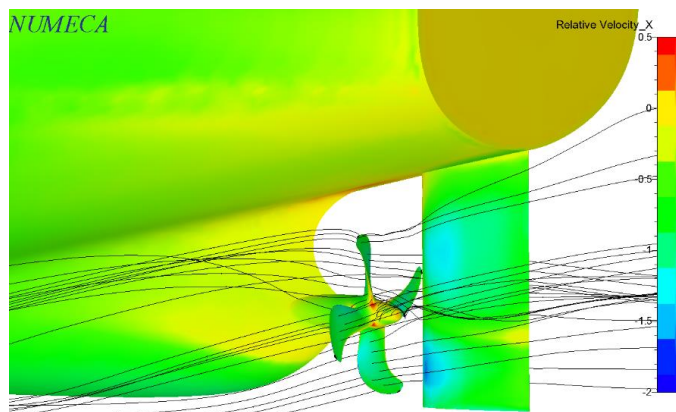
Figure 4.18: Streamline visualization at ship stern

(a) Vortex identification (λ₂ = -50)

(b) Free surface elevation at ship stern

Figure 4.19: Vortex identification (λ₂ = -50) and free surface elevation at ship stern

4.5. Evaluation and discussion

The simulation of propeller behind the hull form, with and without rudder is investigated in this chapter. The interpolation process to find self-propulsion point is also carried out for the case of without rudder. Generally speaking, the result of this simulation *without* rudder is fairly good, even when comparing to experiment result *with* rudder. The difference is around, and less than 5% for the propulsion parameters in behind-condition (thrust deduction, wake fraction, relative rotative efficiency).

When adding a dummy rudder into simulation, there is only one simulation with the propeller revolution (n) same as experiment is carried out (just to see the influence of rudder). The rudder blocks the flow from propeller (called rudder blockage, in terms of physical and numerical blockage [15][16]), modifies the pressure field at stern, consequently, the thrust of propeller increases by 6%, just only 4% difference (comparing to experiment). Some authors also found out this phenomenon [15][16][17], and they pointed that the interaction of rudder to propeller thrust and torque depends on relative location of rudder to propeller. Ship resistance also rises because of rudder resistance, leading to less than 1% difference from experiment. It is noted that, we compare the simulation result with *the experiment with rudder*. There is a consistence in this case (simulation with rudder compared to experiment with rudder), hence, improving of result is reasonable.

In conclusion, considering the complexity of simulation of propeller behind ship, the result obtained is quite good. Besides, regarding practical use, the most difficulty of the simulation is time consumption and computational resources. It takes more than 48 hours to run simulation with 1 propeller revolution on parallel by 96 cores over 3 nodes (32 cores each nodes). The reason is due to Sliding Grid approach, the connection between propeller domain and ship domain needs to be recalculated for each time step. However, with the development of computing technology, this issue could be solve in very near future.

(This page is intentionally left blank)

5. FINAL CONCLUSION AND FUTHER DEVELOPMENT

5.1. Final conclusion

The thesis presents the CFD approach using RANSE solver for propeller calculation, in both case: open water and behind hull. For open water, different methods, different turbulence models are investigated. For propeller behind ship, the simulation with and without rudder are carried out; the propulsion point is also calculated by interpolation.

In term of open water simulation, generally speaking, the result is acceptable comparing with experiment. The difference between CFD and experiment is getting higher for thrust coefficient K_T when advance coefficient J increases (less than 5% difference for small J and around 10% difference for high J). The investigation also points out that Rotating Reference Frame method is the most suitable one for doing open water simulation, considering computational resources and level of accuracy. Using the mesh size around 4 million cells, it takes roughly 16 hours calculation on parallel over 16 cores with very quick convergence of result. For this reason, Rotating Reference Frame method could be applied in practical or daily use, to simulate propeller in open water condition. Regarding turbulence model, two-transport equation model (in eddy viscosity model) k-ω SST or k-ω BSL gives us closest result to experiment. The good result of simulation with Laminar flow and high Reynolds number proves that there are scale effect and large laminar flow areas exist on propeller in open water test.

The self-propulsion simulation (or simulation of propeller working behind ship) shows quite better result. The results of estimation of parameters characterizing "propeller behind ship performance", such as thrust deduction (t), effective wake coefficient (1 - w) or relative rotative efficiency ($η_R$) are good in comparison with experiment (***the experiment is performed with rudder)***: less than 5% difference. By adding a dummy rudder in the simulation, it is found that the ship resistance and propeller thrust increase, leading the estimation of K_T much closer to experiment: only 4% difference. In case of no rudder, with same propeller revolution, the difference of K_T is more than 10%. This is due to in two cases (with and without rudder), we compare with ***"experiment with rudder"***. Then, the influence of rudder to propulsion simulation is proved. Consequently, it is necessary to include rudder in propulsion simulation.

However, the most difficulty of this simulation is computational time. Using Sliding Grid with large number of cells (including full ship, propeller and rudder) is very time and resources consumption. It takes roughly 48 hours running 1 simulation on parallel in 96 cores over 3 nodes.

In conclusion, this thesis investigates many aspects of propeller simulation by CFD approach using commercial ISIS solver. Considering the complexity of propeller geometry and setup of simulation, especially for propeller behind ship using Sliding Grid, the overall result is fairly good. However, because all the investigation, study and simulation are performed in the short time, only four months, there are, of course, many points which could be improved and developed further.

5.2. Further development

As stated above, due to time limitation, the work of this thesis only covers the main and basic points of propeller simulation. When the setups for simulation, computational procedures are investigated in this thesis, and ready to apply; the further steps could be doing much more simulation in detail.

Particularly, in open water simulation, the result of K_T is often under estimation when advance coefficient J increases. One reason for this is explained in this thesis: K_T is getting smaller corresponding with the increase of J. However, it is worth to try finer mesh. This thesis has done the simulation with 9 million cells but the result is not improved. Further investigation can do the simulation with double mesh size, up to 20 million cells. Other solution might be doing many open water simulations. If there are over large numbers of simulations, the difference with experience remains at some certain values, and one can build up the correction factor. Another aspect which should be taken into account is the scale effect, or the existence of large laminar flow area on propeller. Therefore, doing the simulation with transitional turbulence model might be performed. Some authors did this kind of simulation for propeller in open water and getting very good result [18]

Regarding simulation of rotating propeller behind the ship, the interpolation to find propulsion point of the simulation with rudder has not been carried out in this thesis. Hence, it is the first point to consider for further development. Moreover, computational time is still an issue for this simulation and it makes impractical to use. Method to reduce computational time might be studied. Besides, there are some alternative development such as: comparison of result by CFD with body – force (actuator disk) method, making the script for automatization of mesh generation and simulation setup process.

ACKNOWLEDGEMENTS

Nguyen Manh Chien – Rostock, January 2015

REFERENCES

[1] Ferrant P., Seakeeping Lectures 1&2, ECN – EMSHIP 2013/2014.

[2] David le Touzé and Lionel Gentaz, CFD lecture notes, ECN – EMSHIP 2013/2014

[3] D. C. Wilcox, "Turbulence modeling for CFD," tech. rep., DCW Industries, Inc., 5354 Palm Drive, La Cañada, Calif., 1993

[4] Numeca Fine/Marine, Theoretical Background Manual, 2014

[5] Ansys Fluent, Theory guide, 2014

[6] Carlton JS, Marine Propellers and Propulsion 3rd edition, Butterworth-Heinemann; 2012.

[7] ITTC – Recommended Procedures 7.5-02 -03-01.1, Testing and Extrapolation Methods Propulsion, Performance Propulsion Test; 2002

[8] Numeca Fine/Marine, Hexpress manual, 2014

[9] Potsdam propeller test case, http://www.sva-potsdam.de/pptc_data.html, SVA Potsdam

[10] Jinhee Jeong and Fazle Hussain, On the identification of a vortex, Journal Fluid Mechanic (1995), vol. 285, pp. 69-94.

[11] Gert Kuiper, "Paint tests on three propellers for the Leading Edge Project", Leading Edge Deliverable D4, CFD Validation for a Marine MARIN, 2005.

[12] Shin Hyung RHEE and Shitalkumar JOSHI, Computational Validation for Flow around a Marine Propeller Using Unstructured Mesh Based Navier-Stokes Solver, 4th Joint Fluids Summer Engineering Conference, ASME/JSME 2003

[13] LI Da-Qing, Validation of RANS predictions of open water performance of a highly skewed propeller with experiments, Journal of Hydrodynamics, July 2006, Pages 520–528

[14] Michel Visonneau et al, Computation of Free-Surface Viscous Flows around Self-propelled Ships with the Help of Sliding Grids, 2011

[15] A. F. Molland and S. R. Turnock, Marine Rudder and Control Surface, 2006

[16] Sánchez Caja et al, Simulation of the Incompressible Viscous Flow around Ducted Propellers with Rudders Using a RANSE Solver, 2008

[17] Vladimir Krasilnikov et al , A Numerical Study on the Characteristics of the System Propeller and Rudder at Low Speed Operation, Hamburg, 2011.

[18] *Xiao Wang and Keith Walters,* Computational Analysis of Marine-Propeller Performance Using Transition-Sensitive Turbulence Modeling, Journal of Fluids Engineering | Volume 134, Jul 20, 2012